Lab on a Chip

CRITICAL REVIEW

View Article Online
View Journal | View Issue

Cite this: *Lab Chip*, 2026, **26**, 2394

Machine learning-augmented lateral flow assays for point-of-care infectious disease diagnostics

Cagla Parmaksizoglu, [ab] Isil Cakiroglu, [ab] Nazente Atceken, [abcde] Eden Morales-Narváez, [f] Ali K. Yetisen [g] and Savas Tasoglu [*abhijk]

Lateral flow assays (LFAs) are among the most widely used point-of-care (PoC) diagnostic platforms for infectious diseases due to their rapid operation, low cost, and user-friendly architecture. However, conventional LFAs remain limited by analytical sensitivity, qualitative or semi-quantitative outputs, and reliance on subjective visual interpretation. Recent innovations in nanomaterial engineering, signal amplification strategies, and multiplex assay design have significantly improved detection performance across viral, bacterial, and other pathogens. Advanced labels, CRISPR-assisted amplification, and dual-mode sensing formats have expanded the analytical capabilities of LFAs beyond traditional colorimetric designs. Parallel to material and biochemical advancements, AI and machine learning (ML)-based image analysis have emerged as transformative tools for digital LFA interpretation. Smartphone-assisted readers and convolutional neural networks (CNNs) enable objective, quantitative signal extraction, reduce user-dependent variability, and improve detection of weak test lines. These approaches support standardized analysis and scalable disease surveillance. Despite these advances, challenges remain in sensitivity optimization, dataset quality, standardization, and regulatory alignment of ML-enabled diagnostic platforms. Future integration of AI-driven analytics with robust assay engineering is expected to redefine LFA platforms as digitally connected, quantitative, and clinically reliable PoC diagnostic systems.

Received 5th December 2025,
Accepted 16th March 2026

DOI: 10.1039/d5lc01124h

rsc.li/loc

1. Introduction

Infectious diseases persistently challenge global health, significantly burdening public health, social stability, and healthcare systems worldwide.[1,2] These diseases arise from a diverse set of pathogens including bacterial, viral, fungal and parasitic pathogens, each with distinct transmission mechanisms, pathogenicity, and epidemiological patterns.[3–5] Some infectious diseases such as malaria, influenza, and tuberculosis are endemic and continue to impose a heavy disease burden, while others, like Zika virus, Ebola, and SARS-CoV-2, emerge sporadically, often triggering regional or global outbreaks with severe public health consequences.[6,7] The rapid spread of pathogens is driven by factors such as globalization, climate change, urbanization, and antimicrobial resistance, which collectively hinder disease control and prevention efforts.[8,9]

Early and accurate diagnosis is therefore the foundation of effective infectious disease management, enabling timely clinical intervention, guiding appropriate treatment strategies, and preventing further spread within communities.[3] Rapid identification of infectious agents is particularly critical in the case of highly contagious or severe diseases, where delays in diagnosis can lead to widespread outbreaks and increased mortality rates. However, despite the advancements in diagnostic technologies, access to reliable and efficient tests remains limited in many regions, especially in low- and middle-income countries.[8] Healthcare infrastructure in these areas often lacks the resources and technical capabilities to support complex, laboratory-based diagnostic methods, leading to delays in disease detection and treatment.[10]

[a] *School of Biomedical Sciences and Engineering, Koç University, Istanbul, 34450, Turkiye. E-mail: stasoglu@ku.edu.tr*
[b] *Koç University Translational Medicine Research Center (KUTTAM), Koç University, Istanbul, 34450, Turkiye*
[c] *School of Medicine, Koç University, Istanbul, 34450, Turkiye*
[d] *Department of Medicine, Solna (MedS), Division of Dermatology and Venereology, Karolinska Institutet, Stockholm, Sweden*
[e] *Centre for Molecular Medicine, Karolinska University Hospital, Stockholm, Sweden*
[f] *Biophotonic Nanosensors Laboratory, Centro de Física Aplicada y Tecnología Avanzada (CFATA), Universidad Nacional Autónoma de México (UNAM), Querétaro, 76230, Mexico*
[g] *Department of Chemical Engineering, Imperial College London, South Kensington, London, SW7 2BU, UK*
[h] *Department of Mechanical Engineering, Koç University, Istanbul, 34450, Turkiye*
[i] *Koç University Is Bank Artificial Intelligence Lab (KUIS AI Lab), Koç University, Istanbul, 34450, Turkiye*
[j] *Koç University Arçelik Research Center for Creative Industries (KUAR), Koç University, Istanbul, 34450, Turkiye*
[k] *Boğaziçi Institute of Biomedical Engineering, Boğaziçi University, Istanbul, 34684, Turkiye*

To bridge this diagnostic gap, there is an urgent need for cost-effective, scalable, and portable diagnostic solutions that can be deployed in resource-limited environments.[3,11–13] Such technologies should be designed to provide real-time, rapid, accurate, and user-friendly results while minimizing dependence on laboratory facilities and specialized training.[14–19] One of the most promising techniques in this regard is lateral flow assay (LFA), a simple and efficient diagnostic platform that has gained widespread recognition for its applicability in infectious disease detection.[20–22] LFAs are advantageous due to their affordability, ease of use, rapid results, and long-term stability, which make them highly suitable for point-of-care testing in diverse domains.[11,23] Since their introduction to the industry, these devices have been adapted for applications including biomarker detection, food safety assessment, veterinary medicine, and environmental monitoring.[22,24] In the context of infectious disease diagnosis, LFAs offer a practical and scalable approach to improve global health outcomes, particularly in regions where traditional diagnostic methods remain inaccessible or impractical.[25] Despite the widespread adoption of LFA systems, inherent shortcomings such as suboptimal sensitivity, inability to provide quantitative data, and reliance on visual interpretation of results remain significant limiting factors.[26–28] In parallel with recent advances in biosensor technologies, the integration of artificial intelligence (AI), particularly machine learning (ML) algorithms, into diagnostic systems demonstrates that many of these limitations can be overcome.[10,29–34] This review summarizes the current use of LFA systems in infectious diseases and discusses how these systems can be made more robust, reliable, and intelligent through ML-based solutions.

2. Current landscape of lateral flow assays in infectious diseases

LFA is a biosensor platform generally based on antigen–antibody or nucleic acid-based interactions, enabling rapid and cost-effective diagnosis (Fig. 1).[35,36] Its portable structure makes it widely used in the field detection of infectious diseases. LFA systems generally consist of a sample pad, conjugate pad, nitrocellulose membrane, and absorbent pad; however, they can be diversified with different structural designs, such as single-line (sandwich-type), competitive, multiple-line, or microfluidic-based designs, depending on the intended use (Fig. 1).[35,36] LFAs are point-of-care (PoC) systems that detect genetic material or nucleic acid molecules of viruses, bacteria, and other pathogens (Table 1).

2.1. Viral infectious disease diagnosis

Viral infections present unique challenges due to their high transmissibility and capacity for rapid evolution.[37–39] The swift mutation rates of viruses can give rise to new strains that evade existing diagnostic tools and treatments, complicating outbreak control efforts.[40] In this context, LFAs have proven to be invaluable diagnostic methods, offering scalable and rapid solutions.[37] The COVID-19 pandemic underscored their critical role in viral diagnostics.[41–43] SARS-CoV-2 antigen tests, which target the viral nucleocapsid protein, were employed globally to enable mass screening.[44] Their simplicity, affordability, and rapid results enabled decentralized testing in both clinical and non-clinical settings, including workplaces and schools.[45] While reverse transcription polymerase chain reaction (RT-PCR) remains the gold standard, LFAs served as a complementary approach, particularly in low-resource environments where access to advanced laboratory facilities is limited.

A very recent study by Peng *et al.* addresses this issue with a novel nanobody-based LFA for detecting SARS-CoV-2 and MERS-CoV proteins (Fig. 2A).[42] Nanobodies, also known as single-domain antibodies (VHHs) derived from camelids, were chosen due to their small size, high stability and strong antigen-binding affinity, leading to highly sensitive and successful detection. Using single- and dual-format LFAs, the researchers aimed to detect SARS-CoV-2 and MERS-CoV proteins individually and simultaneously. The detection mechanism relies on gold nanoparticle (AuNP)-conjugated nanobodies that capture the target antigens, forming visible bands on the test line. Notably, the researchers demonstrated that their assay could successfully differentiate SARS-CoV-2 from MERS-CoV, ensuring specificity in detecting each virus. Additionally, this is the first reported nanobody-based MERS-CoV LFA and the first nanobody-based sandwich LFA that can be observed with the naked eye. Sensitivity and specificity tests were conducted using the MERS-CoV S1 protein and receptor-binding domain (RBD), with the LOD for the SARS-CoV-2 S1 protein and RBD determined to be 3.27 nM and 0.95 nM, respectively. Similar tests were performed on MERS-CoV strips, where the LOD for the spike protein and RBD were 1.75 nM and 9 nM, respectively.[42]

Sarathkumar *et al.* approached from another perspective by incorporating aptamer-architectured plasmonic nanoenzymes and *para*-phenylenediamine (PPD) as a chromogenic structure to enhance LFA sensitivity and signal strength.[46] AuNP-based nanoenzymes were used for catalyzing the oxidation of PPD to Bandrowski's base (BB), which is a stable and dark brown product that increases the signal intensity while providing stronger contrast against the nitrocellulose (NC) membrane. The PPD-based LFA was later evaluated using SARS-CoV-2 spike protein, and the assay demonstrated a detection limit of 168 pg mL^{-1}, which is more sensitive than that of Peng *et al.*'s approach.[42] Further, this system achieved a 20-fold improvement in sensitivity within 15 minutes.[46] Wang *et al.* also used a competitive aptamer-based LFA for the rapid and quantitative detection of SARS-CoV-2 spike protein (Apt-LFD).[47] Like in all previously mentioned research, AuNPs were used as detector probes and are conjugated to DNA probes for signal generation, and the system achieved a detection limit of 51.81 ng mL^{-1}, with a linear detection range of 0.1–1 μg

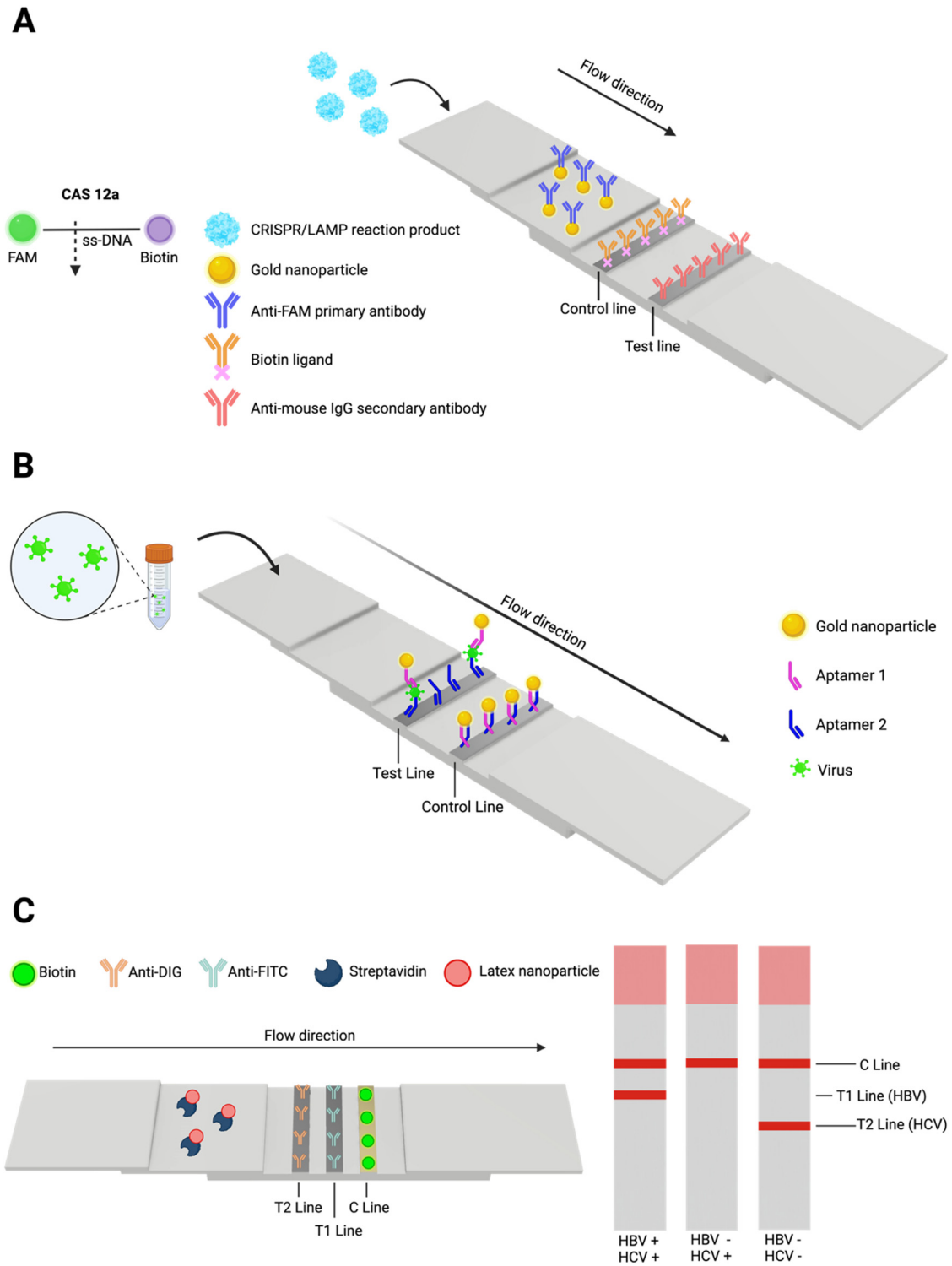

Fig. 1 LFA strip designs. (A) CRISPR/LAMP sandwich-type LFA. CRISPR/LAMP reaction products are placed on the sample pad, where they flow to the conjugate pad to bind to anti-FAM conjugated AuNPs. Depending on the binding, a positive result with two lines (control and test) is visible. A negative result is depicted with a single line on the control line. (B) Sandwich-type aptamer-based LFA for MTB and MAC detection. In the presence of the target virus, AuNP-conjugated aptamer 1 binds to the virus and forms a complex, which is subsequently captured by aptamer 2 at the test line, forming a visible signal. The excess unbound AuNP–aptamer 1 continues to migrate to the control line and is captured to confirm assay function.[35] (C) m-LFA for simultaneous detection of HBV and HCV. The assay utilizes latex nanoparticle-labelled streptavidin as a detection probe which binds to biotin-labelled targets. T1 and T2 test lines are coated with anti-FITC and anti-DIG antibodies to capture HBV and HCV detection complexes, respectively. A control (C) line containing immobilized biotin confirms correct flow and assay validity. Signals from all three lines indicate dual HBV and HCV positivity, only C and T1 lines indicate HBV positive and HCV negative, and finally a single C line indicates a negative result for both infections.[36]

Table 1 Other LFA strategies for detecting bacterial and viral infectious diseases

Disease	Reporter type/probe	Detection element	Assay type	Sample type	Specificity/LOD	References
Tuberculosis	AuNPs	CFP10-ESAT6	LFIA	Sputum	—	83
Dengue	—	DENV1 DENV2 DENV3 DENV4	RT-RPA-LFD	Serum	10 copies per RNA	84
Dengue	IgG	DENV1	NIR-LFA	Serum	Sensitivity 05%	104
Influenza	AuNPs-SA	Influenza A Influenza B	Flu-LAMP-LFA	—	36.1 ng μL^{-1} 36.0 ng μL^{-1}	49
Influenza	—	—	RT-LAMP-LFA	—	Sensitivity 83.5%	105
Influenza		H1N1	LFA-based biosensor		—	85
Influenza	GO-SELEX	H5N2	LFA	—	1.27×10^5 EID_{50} $m^{-1}l$	35
Influenza	—	Influenza A Influenza B	LAMP-LFA	Nasopharyngeal swab	94.10% 96.60%	50
Influenza	—	Influenza A Influenza B	HRP-labelled LFA	Oropharyngeal and nasopharyngeal swab	Sensitivity 77.5%, specificity 99.8% Sensitivity 71.2%, specificity 99.8%	106
Influenza	Quantum dots	Influenza A Influenza B	LFA	Nasopharyngeal swab	Sensitivity 80.9%, specificity 100% Sensitivity 83.7%, specificity 100%	107
Pneumonia	AuNPs	—	CRISPR/Cas9-LFB	Sputum	3×10^0–3×10^6 copies	60
Pneumonia	AuNPs-RSA	—	—	Human serum	—	62
Pneumonia	Nanoparticle	MP	LAMP-LFA	gDNA, Oropharyngeal swab	600 fg of DNA templates	61
Zika virus	EuNPs	—	FICT-LFA	Urine, serum	2×10^4 $TCID_{50}$ mL^{-1}	54
Norovirus	AuNPs	Norwalk virus-like particles				108
Zika virus	Fluorescent	ZIKV NS1	LFA	Serum	0.15 ng mL 1 LOD	53
Gonorrhoeae	Fluorescent	—	Fluorescent-LFA	Genital clinical samples	Sensitivity and specificity of 78.6% and 100% in female vaginal swabs 100% and 89.7% in male urine	109
Chlamydia	—	CPSIT_RS02830 gene	RAA-LFA	—	1×10^0 copies per μL	82
Salmonella	AuNPs	Salmonella spp.: *S. enteritidis*, *S. typhimurium*	RPA-LFA	—	2.8×10^2 LOD 5.9×10^2 LOD 7.6×10^2 CFU mL^{-1} LOD	110
Hepatitis B	SA-GNPs	S gene	PSR-LFB	Blood	5.4 copies per mL LOD	111
Covid-19					High specificity	112
Covid-19	AuNPs	RdRp and ORF8 gene	RT-LAMP-LFA	Swab samples	Sensitivity 95%, specificity 75%	113
Covid-19	Nanobody-AuNPs	SARS-CoV-2 S1, RBD MERS-CoV, RBD	Multiplex LFA	—	LOD: 3.27 nM, 0.94 nM LOD: 1.75 nM, 9 nM	42
Covid-19	—	Cas13a	CRISPR-LFA	—	LOD: 0.05 copies per μL, 100% sensitivity and specificity	114
Covid-19	Oligonucleotide-AuNPs	RdRp gene	RT-RAA-based NALFA	—	LOD: 12 RNA copies per μL, sensitivity 86%, specificity 97%	115
HPV	—	HPV E7 cfDNA	RPA-LFA	Serum	Sensitivity 30.77%, specificity 100%	116
HPV	AuNPs	HPV16 and HPV18	RC-LFA	—	Sensitivity 10 copies per μL	117
HPV	—	HPV16 and HPV18	NALFA	—	LOD: 10 aM	118
HPV	PdRu	HPV16 HPV18	DLFA	—	LOD: 0.93 nM LOD: 0.19 nM	119
Hepatitis B	AuNPs	HBsAg	Laser-assisted LFA	Plasma	—	120

mL^{-1}. This study also further assessed cross-reactivity and stability against other viral proteins such as respiratory syncytial virus (RSV) and human coronaviruses (HCoV-OC43 and HCoV-229E), and the tests confirmed reliable performance over a 16 day period.[47]

Influenza is another respiratory virus where LFAs have made significant contributions. Kim *et al.*[35] developed a novel sandwich-type lateral flow strip biosensor for detecting avian type A influenza (H5N2) whole virus particles using a pair of cognate aptamers. The aptamers were screened using

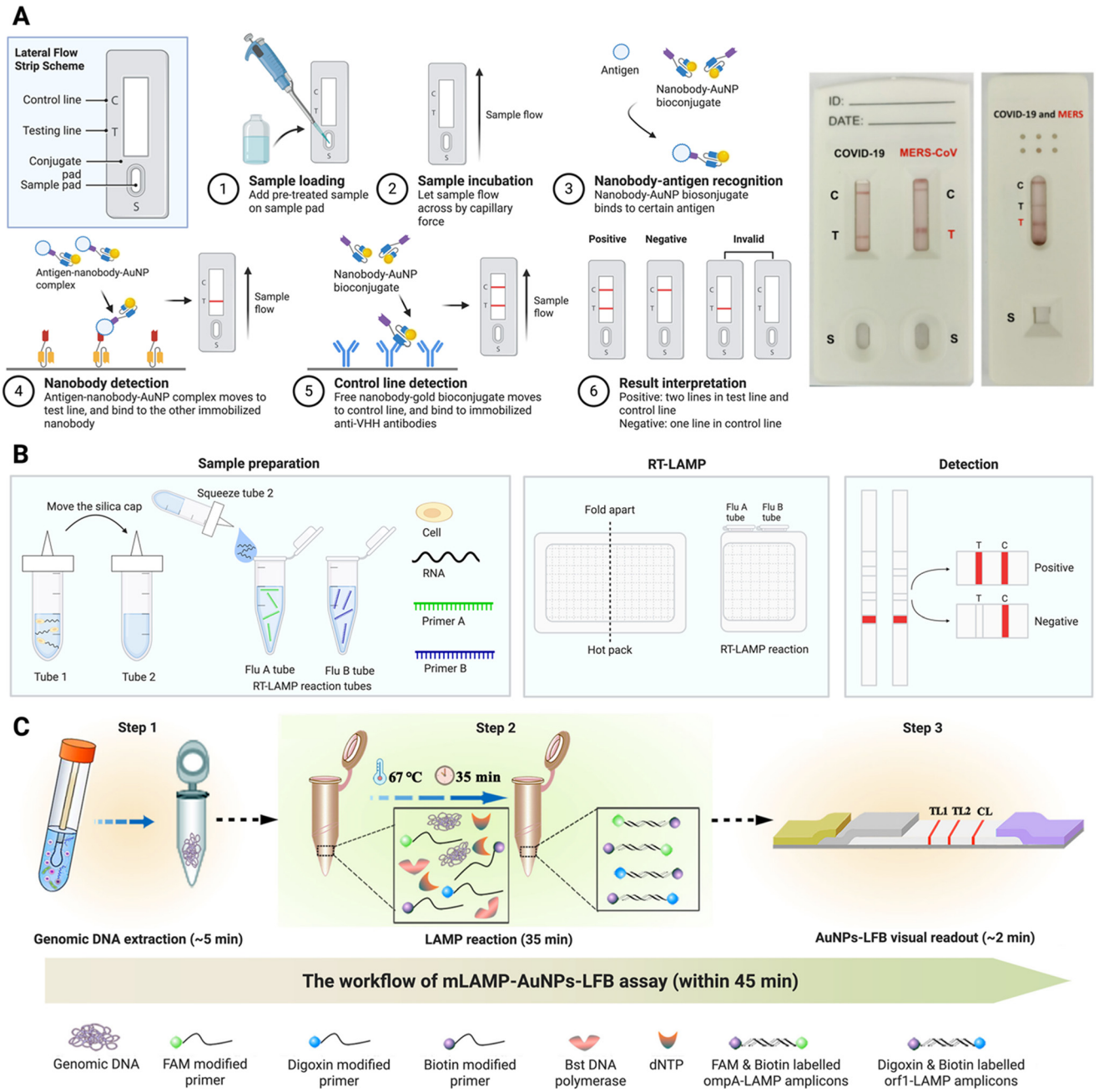

Fig. 2 Layout and working principle of LFAs. (A) Nanobody-based LFA for the detection of SARS-CoV-2 and MERS-CoV proteins. Following sample addition, antigens in the specimen bind to nanobody–AuNP conjugates, forming antigen–nanobody–AuNP complexes. These complexes are captured by immobilized nanobodies at the test line, producing a visible red band. The remaining conjugates then migrate to the control line, where anti-VHH antibodies bind to excess nanobody–AuNPs, confirming assay validity. The presence of two red lines (test and control) indicates a positive result, whereas a single line at the control line denotes a negative result. Example LFA cassettes for COVID-19 and MERS-CoV are shown in the next panel. Adapted with permission from ref. 42. Copyright 2025, *ACS Synthetic Biology*. (B) Flu-LAMP-LFA for influenza virus detection. Lysis and elution are performed using the squeeze method, with one drop of sample added to each of the flu A and flu B tubes. Nucleic acid amplification is achieved by placing the tubes between a preheated, half-folded hot pack. Following amplification, LFA strips are analyzed where the appearance of two red lines (test and control) indicates a positive result. In contrast, a single red line at the control depicts a negative result. Adapted from ref. 49. Copyright 2022, Minju Jang, SeJin Kim, Junkyu Song, and Sanghyo Kim, published by *Analytical and Bioanalytical Chemistry* under the license indicated. (C) m-LAMP assay combined with AuNP-based lateral flow biosensor (AuNP-LFB) for the rapid detection of *C. trachomatis* and *N. gonorrhoeae*. The assay is completed within 45 minutes and consists of three main steps. First, genomic DNA is extracted from the sample. Second, a LAMP reaction is performed at 67 °C for 35 minutes using primers labelled with FAM, digoxigenin, or biotin along with Bst DNA polymerase and dNTPs. This results in the amplification of target genes tagged with specific reporter molecules. The amplified products are then applied to an LFB for visual detection. The appearance of red bands at TL1 and TL2 indicates the presence of specific targets, while the CL confirms successful assay performance. Adapted from ref. 67. Copyright 2023, Xu Chen, Qingxue Zhou, Wei Yuan, Yuanfang Shi, Shilei Dong and Xinhua Luo, published by *Frontiers in Cellular and Infection Microbiology* under the license indicated.

the graphene-oxide SELEX (GO-SELEX) method to enable high specificity and binding to different sites on the target virus. J_3APT and JH_4AP aptamers, which were found to be working as a cognate pair that can simultaneously bind to different sites of the target virus, were selected and extensively characterized using techniques such as Förster resonance energy transfer (FRET), surface plasmon resonance, confocal laser scanning microscopy, and circular dichroism spectroscopy to confirm strong and specific binding to H5N2 virus and were used as capturing aptamer and secondary aptamer, respectively. They observed that as the second aptamer conjugated AuNP concentration increased; the signal intensity also increased, even though it made the washing step difficult, which resulted in high background noise. The sensor demonstrated a detection limit of 1.27×10^5 EID_{50} ml^{-1} in buffer and 2.09×10^5 EID_{50} ml^{-1} in spiked duck feces, which enables detection with the naked eye.[35]

Reverse transcriptase loop-mediated isothermal amplification (RT-LAMP) can be used for simultaneous detection and subtyping for influenza viruses.[48] In one study, Jang *et al.*[49] published a LAMP-LFA platform for detecting both influenza A and B viruses using a combination of RT-LAMP (Fig. 2B). The platform consists of three steps: sample preparation, RT-LAMP, and LFA detection. Jang and colleagues also amplified RT-LAMP and optimized it with primers specifically targeting conserved regions of the matrix gene and NS1 gene. They further continued with specificity tests, which showed no cross-reactivity with SARS-CoV-2, coronavirus NL63, coronavirus OC43, enterovirus D68, or respiratory syncytial virus. Further, this method introduced chemical hot packs as a heat source, replacing thermocyclers and making it portable and electricity-free. The LFA showed clear and accurate results within minutes, with a detection limit of 10^4 for influenza A and 10^5 for influenza B.[49] In another recent study by Jang *et al.*,[50] a multiplex LAMP and LFA (LAMP-LFA) was used for simultaneous detection of influenza A and B. This approach targets conserved genetic regions within segment 7 of influenza A and the nucleoprotein gene of influenza B. Primers labelled with biotin, FAM, and DIG were used which allowed simultaneous detection of both viruses on a single LFA strip, and a high signal strength and minimal non-specific interaction set was selected for the two virus types. The assay demonstrated a sensitivity of 94.1% for influenza A and 96.6% for influenza B, with an overall specificity of 98% for negative samples. They compared their results with that of a commercially available and reliable test, Allplex Respiratory Panel 1, and observed that the detection limit of their proposed method was slightly higher. Further, their assay demonstrated exceptional specificity and did not display any cross-reactivity with other respiratory viruses such as coronaviruses, adenoviruses, and respiratory syncytial viruses.[50]

LFAs have also been utilized for detecting dengue, Zika virus (ZIKV), hepatitis B, and human papillomavirus (HPV). Dengue virus, a rapidly spreading arboviral disease, consists of four serotypes (DENV1, DENV2, DENV3, and DENV4), and differentiating these serotypes is crucial for effective clinical management, epidemiological surveillance, and outbreak monitoring. To address the limitations of current diagnostic tools such as PCR and enzyme-linked immunosorbent assay (ELISA), Lai *et al.*[51] developed a dengue NS1 multiplex LFA for the simultaneous detection and serotyping of the dengue virus in human serum and infected mosquitoes. A serotype-cross-reactive antibody was paired with four serotype-specific antibodies and is utilized for the design of the assay. The multiplex LFA exhibited high sensitivity, with detection rates of 90.0% for DENV1, 88.24% for DENV2, 82.61% for DENV3, and 83.33% for DENV4 clinically. Specificity tests revealed minimal cross-reactivity with other flaviviruses such as ZIKV with values ranging from 96.13% to 99.39%. To further assess accuracy, researchers evaluated the assay using clinical serum samples from suspected dengue patients, where it exhibited an overall accuracy of 89.84% and a positive predictive value of 94.97%.[51]

In a similar study, Trakoolwilaiwan *et al.*[52] developed a thermochromic LFA for detecting the DENV2 NS1 protein by exploiting the photothermal properties of magnetic nanoparticles and AuNPs. Various photothermal nanomaterials were tested for heating efficiency, with 12 nm gold nanospheres showing the best performance. The optimized LFA achieved a LOD of 1.56 ng mL^{-1}, which is four times lower than that of conventional LFAs (6.25 ng mL^{-1}). Notably, a visible colour change provided a semi-quantitative readout: a red signal appeared at concentrations below 1.56 and 12.5 ng mL^{-1}, while higher concentrations produced a greenish blue colour. This visual distinction allows users to estimate viral load without requiring digital image processing or specialized analytical tools, thereby reducing the cost of the assay.[52] Accurate differentiation between ZIKV and DENV is crucial for effective diagnosis and management since these two have close antigenic similarity. A paper published in 2019, which utilizes a smartphone-based fluorescent LFA that is designed to detect ZIKV NS1 protein, demonstrated low cross-reactivity towards DENV.[53] With this outcome, accurate differentiation between ZIKV and DENV was possible. Their system employs a 3D-printed smartphone attachment integrated with external optical and electrical components, minimizing both the cost and the complexity. Quantum dot microspheres were used as fluorescent probes to amplify the detection of ZIKV NS1 within 20 minutes, and the system showed excellent performance with a detection limit of 0.045 ng mL^{-1} in buffer and 0.15 ng mL^{-1} in serum.[53]

It was previously reported by Nguyen *et al.*[54] that a peptide aptamer was able to distinguish ZIKV from DENV using fluorescence-linked immunosorbent assay (FLISA), and they developed an antibody-free diagnostic system using those peptide aptamers specifically designed to target the ZIKV envelope protein. The identification and optimization of the peptide aptamers were conducted through *in silico* modeling and binding affinity analysis, with the B2.33-P6.1 peptide pair selected for its strong binding affinity to ZIKV. The assay's LOD was 2×10^4 $TCID_{50}$ mL^{-1} in tissue culture samples, with

results available within 20 minutes.[54] Despite the smartphone-based LFA offering higher sensitivity, portability, and cost-effectiveness, the FLISA with peptide aptamers represents an innovative antibody-free alternative with specificity toward the ZIKV envelope protein.

In 2020, Bai *et al.*[55] incorporated recombinase-aided amplification (RAA) and a lateral flow dipstick to detect hepatitis B virus (HBV). They have developed two RAA-based assays: an internal-controlled (IC) duplex real-time RAA using a portable fluorescence detection device, and an instrument-free visual detection method utilizing a lateral flow dipstick. The IC is utilized for preventing false negatives and for real-time monitoring of the amplification, and the duration of the assay takes less than 40 minutes at an optimum temperature of 39 °C. Both assays demonstrated high sensitivity and specificity upon clinical testing, with the duplex RAA assay achieving 97.18% sensitivity and 100% specificity, while the RAA-LFD assay showed 95.77% sensitivity and 100% specificity. Both methods were able to detect HBV DNA across multiple genotypes such as B, C, and D with a detection limit as low as 10 IU mL^{-1}.[55]

In another similar study by Zhang *et al.*,[56] an LFA system based on recombinase polymerase amplification (LF-RPA) is used for the detection of HBV. A highly conserved region of the HBV genome spanning nt908-1700 was selected as the target region. The forward and reverse primers were designed at positions nt1175-1204 and nt1300-1329, respectively, while the probe was located between nt1240 and nt1288. The reverse primer was biotin-labelled, and the probe was modified with a 5′ FAM label, an internal tetrahydrofuran (THF) residue for cleavage, and a 3′ C3 spacer, enabling dual-labelled amplicon generation that is compatible with LFA detection. The primer and probe set were designed using the TwistDx RPA kit, and BLAST (Basic Local Alignment Search Tool) was used for specificity analysis of the primers and the probe. The assay operated at an optimal isothermal temperature (37 °C) and achieved a limit of detection of 10 copies per μL, and no cross-reactivity was observed with other common pathogens such as hepatitis C (HCV), DENV, and human immunodeficiency virus (HIV).[56] Guo *et al.*[36] approached from a different perspective, introducing a multiplex LAMP (m-LAMP) with lateral flow detection for simultaneous HBV and HBC detection. The m-LAMP was designed to detect conserved regions of HBV polymerase and surface genes as well as HCV 5′-UTR. The assay operates at an optimized temperature of 65 °C and can be completed within 25 minutes. The design of the strip differs from the traditional LFA style by having a control line, a test line for HBV and a test line for HCV. Sensitivity analysis showed that the m-LAMP-LFA assay could detect as low as 10 genomic copies per reaction for HBV and 1000 genomic copies per reaction for HCV. The assay also demonstrated high specificity with no cross-reactivity with other hepatitis viruses or common bloodborne pathogens. One key innovation of this study is the development of a custom portable heating device, which eliminates the need for a laboratory-based thermal cycler. However, despite having high specificity, they mentioned that minor signal intensity variation could affect the results, therefore opening an improvement in this area.[36]

HPV is another infectious disease that can be detected using advanced LFA methods.[57] For the detection of HPV genotypes 16 and 18, Li *et al.*[58] proposed a dual-readout differential LFA that integrates photoelectrochemical (PEC) and photothermal signal amplification strategies. The system utilizes a paper-film-based chip embedded with a $CuCo_2S_4$/$ZnIn_2S_4$ heterostructure to enhance photoinduced charge separation and interfacial electron transfer. Upon target recognition, CRISPR-Cas12a-mediated cleavage induces conformational DNA changes that regulate the accumulation or release of Au-PDA nanoparticles at the electrode surface. The presence of Au-PDA modulates the PEC current by impeding charge transfer and generates a proportional photothermal response under near-infrared radiation. Notably, the reciprocal variation of PEC and photothermal signals enables internal cross-validation of results, which reduces reliance on subjective visual interpretation and enhances analytical reliability. Great sensitivity with detection limits of 0.21 pM for HPV-18 and 42.92 pM for HPV-16 was achieved, making the assay highly effective for early HPV detection.[58] In contrast, Xiao *et al.*[59] developed a gold–palladium–platinum (Au@PdPt) nanoparticle-based LFA for dual-mode detection of HPV genotypes 16 and 18. Different from that of Li *et al.*,[58] this approach utilizes a dual-target DNA–RNA hybridization combined with an Au@PdPt-mAb probe that allows both qualitative visual detection and semi-quantitative analysis. For quantitative readout, immunostrips were placed in a simple 3D-printed bracket and imaged using a smartphone camera, after which the grayscale intensity of the test lines was extracted using ImageJ software. This standardized smartphone-based imaging setup improved signal reproducibility and enabled semi-quantitative analysis beyond naked-eye interpretation. The assay showed significant sensitivity, achieving a visual detection limit of 0.007 nM for HPV-16 and 0.01 nM for HPV-18. The semi-quantitative detection limits were 0.05 nM and 0.02 nM for HPV-16 and HPV-18, respectively.[59]

The key differences between these methods lie in their detection mechanism and signal amplification strategies. The PEC-photothermal LFA employs CRISPR-Cas12a enzymatic cleavage, which leads to highly specific signal transduction through photoelectric and photothermal dual-signal interaction, while the Au@PdPt LFA relies on enhanced catalytic activity of trimetallic nanoparticles, enabling colorimetric detection and smartphone-assisted qualification. In terms of sensitivity and performance, Li *et al.*'s proposed method demonstrated ultra-high sensitivity in the pM range, whereas Au@PdPt, even though it is less sensitive in the nM range, it is still significantly more effective than traditional AuN-based LFAs. The PEC-photothermal approach is ideal for highly precise HPV detection, while the Au@PdPt system provides

a more practical, rapid, and portable solution, which makes it better suited for large-scale screening.[58,59]

2.2. Bacterial infectious disease diagnosis

Zhu *et al.*[60] developed a CRISPR/Cas9-based lateral flow biosensor (CRISPR/Cas9-LFB) for rapid and accurate detection of *Mycoplasma pneumoniae* (MP). This biosensor combines CRISPR/Cas9 technology with RPA to achieve a sensitivity of as low as 3 copies while completing the entire detection process within 30 minutes. The system demonstrates exceptional accuracy with 100% consistency when tested on 123 clinical sputa and eliminates false positives caused by primer dimers or non-target interactions. Unlike traditional PCR-based methods, this system operates efficiently at room temperature without requiring specialized equipment, which makes it suitable for PoC devices in resource-limited settings.[60] In another study on detecting MP, Wang *et al.*[61] reported a LAMP combined with a nanoparticle-based lateral flow biosensor (LAMP-LFB). This assay integrates LAMP technology with LFA for rapid and sensitive detection and specifically targets the P1 gene of MP using six primers by achieving a limit of detection of 600 femtograms (fg) in pure cultures with no cross-reactivity with other pathogens. The working principle of the assay is simple: it requires a heating block at 65 °C for amplification, and the results can be observed within 2 minutes. The assay was tested on 209 clinical samples, and their developed biosensor demonstrated higher sensitivity with a 47.8% detection rate compared to real-time PCR.[61]

In 2019, Tomás and colleagues[62] proposed a new method to diagnose *Pneumocystis jirovecii* pneumonia (PcP), which is a fungus infection that can cause fatal pneumonia. Recombinant synthetic antigens of *P. jirovecii*'s Msg and Kex1 with AuNPs were used to improve the detection of specific antibodies in human sera samples. The results showed excellent visual results with positive sera forming distinct control and test lines within 10 minutes.[62]

Other than pneumonia, LFAs have been used in the diagnosis of tuberculosis. One example is a highly specific and sensitive diagnostic assay using m-LAMP combined with a nanoparticle-based lateral flow biosensor (mLAMP-LFB) specifically targeting two *Mycobacterium tuberculosis* complex (MTBC) specific genes, IS6110 and gyrB.[63] The system operates under isothermal conditions at 65 °C for 40 minutes followed by a lateral flow detection in 2 minutes. The LoD was estimated at 100 fg of DNA in pure culture, and the specificity tests confirmed 100% accuracy with no cross-reactivity with other bacterial species or non-tuberculous mycobacteria (NTM). They further tested their assay using 60 suspected TB patient samples and compared the mLAMP-LFB results with those of traditional methods, including culture, smear microscopy, and the GeneXpert MTB/RIF assay. Their proposed method showed 100% accuracy and outperformed smear microscopy.[63] Recently, Chen *et al.*[64] developed a duplex RAA-lateral flow dipstick (RAA-LFD) assay for the rapid and specific detection of *M. tuberculosis* (MTB) and *M. avium* complex (MAC) to diagnose tuberculosis. The assay targets the MTB-specific IS6110 gene and the MAC-specific DT1 gene, which allows simultaneous differentiation of tuberculosis from MAC infections. The amplification reaction occurs at a constant temperature of 37 °C within 20 minutes, and the results can be visually interpreted using a lateral flow dipstick. Specificity tests showed no cross-reactivity with MTB or other common respiratory pathogens, indicating a very high diagnostic accuracy. Sensitivity analysis demonstrated that the duplex RAA-LFD assay achieved organism-specific detection limits, with a limit of detection of 6.2×10^3 CFU mL^{-1} for MTB and 8.4×10^2 CFU mL^{-1} for MAC. In clinical evaluation using Xpert/MTB RIF as the reference standard, the assay achieved a sensitivity of 92.86% and a specificity of 93.75% for MTB detection. RAA-LFA also identified MTB cases that smear microscopy and culture have missed, indicating its potential for tuberculosis diagnosis, especially in resource-limited environments.[64] Similarly, Gan *et al.*[65] introduced the ERA-CRISPR/Cas12a system as a novel approach for detecting MTB while integrating enzymatic recombinase amplification (ERA) with CRISPR/Cas12a-mediated detection. This system targets the IS1081 gene, ensuring broader strain coverage compared to IS6110-based methods. The ERA step enables rapid DNA amplification at a constant temperature to eliminate the need for thermal cycling. The Cas12a enzyme binds to the target sequence upon successful amplification and triggers a collateral cleavage of a fluorescent or lateral flow probe to generate a signal. The fluorescence-based detection system has observed an LOD as low as 9 copies per μL, while the lateral flow system had an LOD of 90 copies per μL. Additionally, its cost-effectiveness, with an estimated cost of $7 per test, makes it an alternative for widespread implementation.[65]

Building on the advancements in LFA strategies, other innovative approaches have also emerged for diagnosing different bacterial infectious diseases. As one of the most common bacterial sexually transmitted infections (STIs), *C. trachomatis* remains a major global health concern, especially in underdeveloped regions where access to complex diagnostic tools is limited. One promising study to overcome this case utilized LAMP and AuNPs with LFA to detect *Chlamydia trachomatis*.[66] In this study, the assay targets the ompA gene. The entire detection process is completed within 60 minutes, including genomic DNA extraction (15 minutes), amplification (35 minutes), and lateral flow visualization (2 minutes). The designed system denotes high sensitivity, detecting 50 copies per mL of *C. trachomatis* DNA, with 100% specificity confirmed against other pathogens.[66] The same research group also tried to detect *Neisseria gonorrhoeae* using the same system as previously discussed. However, the strategy was inadequate to simultaneously detect *C. trachomatis* and *N. gonorrhoeae*; therefore, in 2023, they integrated m-LAMP with AuNPs for the rapid and visual detection of *C. trachomatis* and *N. gonorrhoeae*. The m-LAMP-AuNPs LFB was designed to target the ompA gene of *C.*

trachomatis and the orf1 gene of *N. gonorrhoeae*. The optimal reaction conditions were determined to be 67 °C for 35 minutes. The entire detection process, including crude DNA extraction (~5 minutes), m-LAMP amplification (35 minutes), and lateral flow detection (~2 minutes), can be completed within 45 minutes. The assay demonstrated a detection limit of 50 copies per test with no observed cross-reactivity with other pathogenic bacteria, which ensures high specificity and accurate differentiation between *C. trachomatis* and *N. gonorrhoeae* (Fig. 2C).[67] In addition, bacterial vaginosis has been detected through disposable devices using GO as a revealing agent of immunocomplexes. Sialidase, a biomarker overexpressed in bacterial vaginosis infection, was employed as a target analyte in this biosensing approach. In fact, GO was discovered to have a high affinity against antibodies; as a consequence, GO quenches the fluorescence of fluorescence-labelled antibodies that do not form immunocomplexes *via* FRET. In contrast, those fluorescence-labelled antibodies that set up immunocomplexes create a spacer between GO and the respective fluorophore; therefore, FRET is hindered and such a fluorescence is not quenched. In these devices, a detection zone is coated with GO to reveal the presence of overexpressed sialidase, whereas a control zone is included to validate and normalize the results of the test. The disposable device was proven useful with clinal samples, offering a promising PoC platform for bacterial vaginosis diagnosis.[68]

2.3. Other infectious diseases

Beyond viruses and bacteria, infectious diseases are caused by four other major classes of pathogens: protozoan parasites, helminths (parasitic worms), fungi, and prions. Among these, protozoan parasitic infections stand out as the most perilous ones. Nearly two-thirds of all deaths caused by other pathogens each year are attributable to protozoa, and malaria alone accounts for the majority. The 2024 World Malaria Report tallied 263 million clinical cases and 597 000 deaths in 2023, almost all in children under five in the African region.[69] A vector-borne disease, visceral leishmaniasis, although far less common, is even more lethal.[70] Without treatment, its case fatality exceeds 95%.[70] Caused by contact with faeces/urine of infected blood-sucking triatomine bugs, Chagas disease still kills about 10 000 people annually and leaves many more with irreversible cardiomyopathy or neurological alterations.[71] Considering these, an early detection test is critical for reducing the death rates globally, especially in endemic regions. For this purpose, Lin *et al.* developed an RAA-LFA assay targeting the *Plasmodium* 18S rRNA, enabling the rapid detection of the parasite responsible for malaria.[72] Using a commercially available RAA test, 15 minutes of incubation at 37 °C followed by a 3 minute strip read-out is conducted for detection of a single plasmid copy. Their assay's sensitivity was 1 copy per μL of recombinant plasmid. They collected blood samples of patients that were infected with *P. falciparum*, *P. vivax*, *P. ovale*, and *P. malariae*, and their corresponding sensitivities were 0.1 pg μL^{-1}, 10 pg μL^{-1}, 10–100 pg μL^{-1}, and 100 pg μL^{-1}, respectively.[72] Targeting the same rRNA, Assefa *et al.* designed RPA-LFA for the specific detection of malaria.[73] Their main goal was to differentiate between *Plasmodium* species rapidly and accurately. Compared with that of Lin's group, RPA-LFA's LoD falls behind, with a detection limit of 10 copies per μL. However, Assefa's longer (~40 minutes), slightly less sensitive workflow fills a crucial niche by reliably discriminating the low-density *P. malaria* infections that pan-plasmodium rapid tests often miss, and its streamlined primer-probe design could be adapted to simple PoC platforms.[73]

The mini-dbPCR-NALFIA platform that van Dijk *et al.*[74] introduced is a simplified molecular diagnostic system that combines direct-on-blood PCR amplification with nucleic acid lateral flow immunoassay (NALFIA) detection, thereby integrating molecular sensitivity with LFA-based visual readout. Unlike conventional PCR approaches, the assay does not require prior DNA extraction. Instead, for the detection of *Leishmania infantum* and *L. donovani* parasites, a limit of detection of 500 and 650 parasites, respectively, was achieved by using only 2.5 μL of EDTA blood.[74] The labelled amplicons are subsequently detected on a dipstick *via* antibody-mediated capture, enabling rapid visual interpretation similar to that of standard LFAs. In a clinical evaluation with 246 Spanish samples, it achieved 95.8% sensitivity and 97.2% specificity, outperforming the widely used rK30 Kalazar Detect strip. To further test their sensitivity, malaria samples were utilized, and pooled 87.9% sensitivity. With a cost of roughly USD 3 and assay time under 1 hour, this developed LFA offers a robust, field-deployable alternative for monitoring visceral leishmaniasis in resource-limited environments.[74] A very recent study conducted by Argentinean researchers has demonstrated that the detection of *T. cruzi* for Chagas disease was possible by a single-step, a 15 minute IgM-based LFA using the antigen CP4.[75] Newborn sera from 28 infected infants were collected, and their LFA correctly identified 9 of 11 congenitally infected cases and all 17 uninfected, achieving 81.8% sensitivity and 100% specificity.[75]

3. Why integration with ML is indispensable?

LFA technologies are widely used in the field diagnosis of infectious diseases due to their rapid, portable, and cost-effective nature. However, traditional LFAs heavily rely on visual interpretation of their results.[76,77] This leads to user interpretation discrepancies, particularly in weakly positive cases such as low signal intensity or blurred bands, limiting the sensitivity and specificity of test results. These limitations negatively impact diagnostic reliability in the field and make standardization of results difficult. ML offers critical tools to overcome these challenges.[31] ML is a set of algorithms capable of automatically recognizing patterns in data, classifying them, and solving regression problems.[29–31] The

most used ML techniques in LFAs include convolutional neural networks (CNNs), support vector machines (SVMs), random forest, and long-short-term memory networks (LSTMs).[29,31] In general, artificial neural networks and random forest are widely employed in classification and regression tasks, whereas SVMs are commonly deployed in classification approaches.[78] CNNs excel at detecting color changes and shape variations in test bands, particularly in image-based data.[29] By evaluating the relationship of each pixel in an image to its surrounding pixels, CNN models can distinguish features such as band intensity and position with high accuracy. Thus, even low-contrast signals that are invisible to the human eye can be successfully identified. SVMs are typically used on datasets that contain a small number of high-quality features.[29] After extracting features such as color intensity, bandwidth, and position, SVMs can effectively separate these data for positive/negative classification. SVMs also offer robust results on complex LFA data thanks to their ability to model linear and nonlinear decision boundaries.[29] The random forest algorithm is an ensemble learning method that works by combining multiple decision trees.[29] This method is powerful against noise in the data and can prevent model overfitting, resulting in more robust classifications. Random forest reduces error rates by modeling variations in LFA data due to different test conditions. LSTM are used in the analysis of time-series data.[27] Dynamic parameters such as sample flow rate and signal generation time are important in LFA tests. LSTM optimizes the testing process by modeling such time-dependent data and enabling early diagnosis.[27] With these techniques, ML algorithms eliminate visual reading errors and enable quantitative evaluation of LFA results. Furthermore, thanks to automatic error detection and quality control mechanisms, some problems caused by misuse, such as faint or missing lines, misaligned bands, or smeared test areas, can be identified early.

Furthermore, ML-powered LFA systems can transfer the acquired data to central health information systems *via* smartphones and cloud-based platforms.[79,80] This enables big data analytics, epidemiological modeling, and real-time outbreak monitoring.[17,30,81] ML plays a critical role in tracing transmission routes, identifying new variants, and optimizing the timing of public health interventions by discovering patterns in these large and heterogeneous datasets.[30]

4. ML–LFA integration: current developments and inspiring applications

In recent years, numerous applications have been reported in the literature where LFAs are combined with ML algorithms to increase sensitivity, specificity, and objectivity of results.[31] This combination has enabled the development of highly accurate diagnostic systems not only in laboratory settings but also in the field.[30] Even though conventional LFAs are practical, simple, and inexpensive, several shortcomings still constrain their clinical and epidemiological impact. Because most of the strips rely on naked-eye detection,[65,67,82–85] they typically yield only a binary yes or no results rather than an analyte concentration,[29] so physicians cannot measure pathogen load or monitor treatment. Passive capillary flow, short optical path-lengths, and unamplified colour labels also make the LFAs less sensitive than traditional immunoassays, while saturation of the test line constraints the dynamic range once colour density maxes out.[29,86,87] Further, multiplexing more than three or four targets on one strip is awkward, both because coloured labels may overlap on the NC membrane and because competitive formats can look blank when they are actually positive, which confuses users (Fig. 4A).[88] The cassette that the strips are put into does not have connectivity, so results are not time-stamped or geo-tagged for public health surveillance.[86]

With the advancements in ML, more work has started to rely on detecting diseases with algorithms.[31] ML methods, mainly CNNs or transformer models, have closed these gaps almost point-for-point.[34] To address these gaps, numerous researchers have employed different models to enhance the qualitative results of LFAs; inspiring examples are summarized in (Table 2).[29,80] One very recent research conducted by Davis and Tomitaka[29] has boosted the quantitative results by developing a smartphone-based ML pipeline that converts the qualitative read-out of COVID-19 antigen LFAs into quantitative classification (Fig. 3A). The authors assembled 2586 photographs, which were taken in a box made from a white foam-core board to limit outside influences, of strip tests spanning 0–7.4 ng of SARS-CoV-2 nucleocapsid protein, later applied extensive data augmentation, and compared five different algorithms. Their CNN model, which was based on LeNet-5 architecture, has 2 convolutional layers followed by an average pooling layer, 2 dense layers with ReLu activation function, a final dense layer with SoftMax activation function, and the model was compiled using Adam optimizer. With this model, the researchers obtained the highest accuracy (95.8%), narrowly outperforming a random-forest ensemble (93.7%), while SVM, *k*-nearest neighbor, and single decision tree models lagged below 83%. For the resolution studies, random forest has been shown to excel on very low-resolution inputs ($\leq 32 \times 32$ pixels), whereas CNN's accuracy rises monotonically with pixel count, peaking at 128 × 128 pixels. Color space comparison, where the colors are represented as numbers, also showed that raw RGB images were sufficient on LFA image classification.[29] Tong *et al.* approached from another perspective for COVID-19 detection by engineering an ML-assisted, polydopamine-nanoparticle (PDA) colorimetric LFA to quantify SARS-CoV-2 neutralizing antibodies at the PoC. The PDA cores were encapsulated in polymer-silica shells, PEGylated, and co-conjugated with spike-protein RBD and mouse IgG, producing fourfold stronger visible absorbance than AuNPs labels. ACE2 was immobilized on the test line and anti-mouse IgG on the control line, yielding a LoD of 160

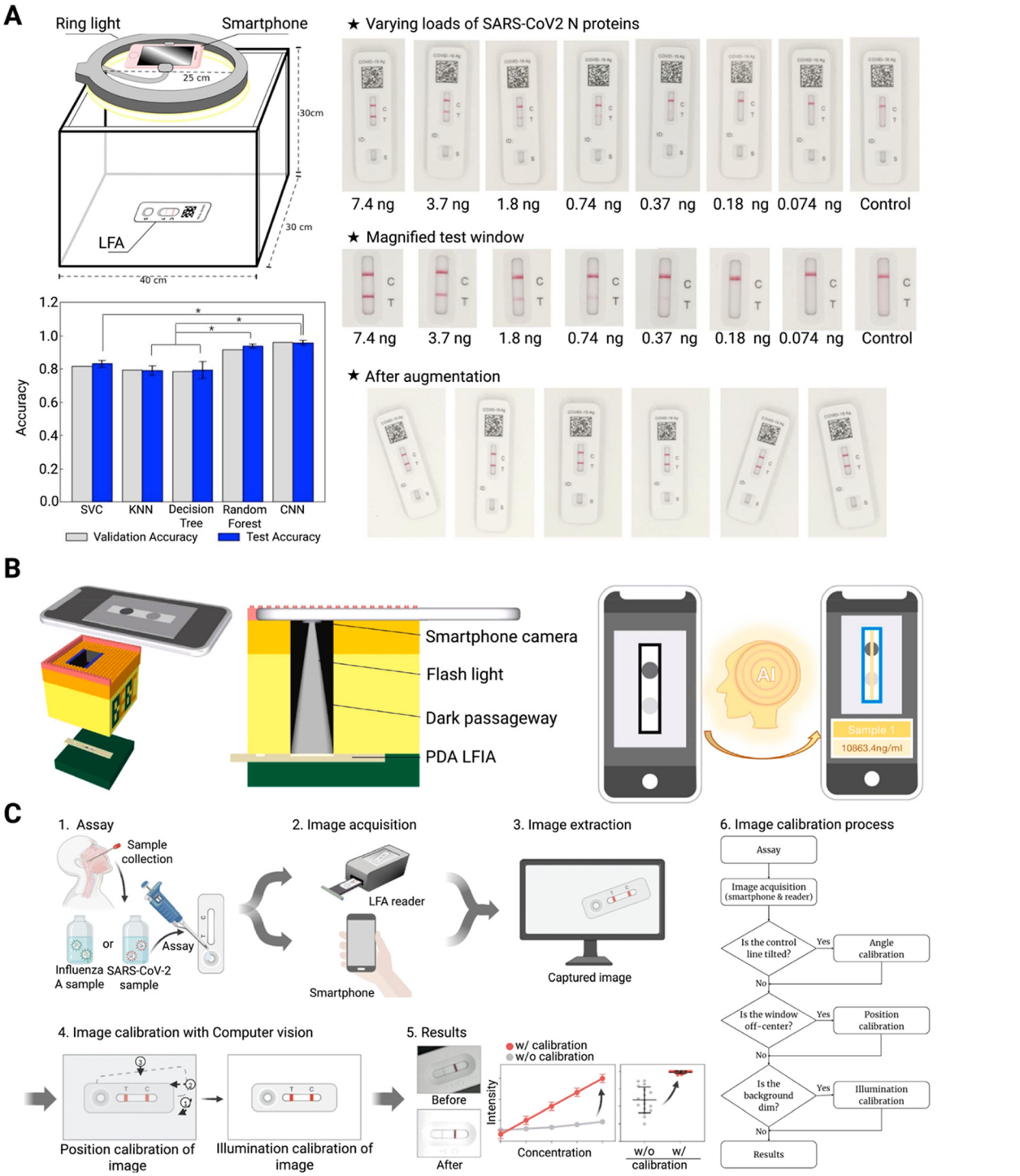

Fig. 3 Schematic representations of ML models for LFA infectious disease detection. (A) Smartphone-based quantification of LFAs. Images of LFA strips were captured using a ring light mounted on a white foam-core photography box to minimize ambient light interference. A smartphone, positioned at the center of the ring light, was used to photograph the strips. The captured images were analyzed, and low-quality photos were excluded for training. LFA tests were then conducted with varying concentrations of SARS-CoV-2 N protein (0.074–7.4 ng), and to simulate real-world variability, multiple image augmentations were applied to the captured strips. Various ML and DL models were later evaluated for classification performance, with CNN and random forest models outperforming the others. Adapted from ref. 29. Copyright 2025, Anne M. Davis and Asahi Tomitaka, published by *Biosensors* under the license indicated. (B) AI-assisted colorimetric lateral flow immunoassay for sensitive and quantitative detection of COVID-19 neutralizing antibody. Adapted from ref. 89. Copyright 2022, Haoyang Tong, Chaoyu Cao, Minli You, Shuang Han, Zhe Liu, Ying Xiao, Wanghong He, Chang Liu, Ping Peng, Zhenrui Xue, Yan Gong, Chunyan Yao, and Feng Xu, published by *Biosensors and Bioelectronics* under the license indicated. (C) CV-assisted LFA analysis system for improved diagnostic accuracy for influenza and SARS-CoV-2. The collected sample (either influenza A or SARS-CoV-2) is applied to the assay, where image acquisition is performed using either a smartphone or a dedicated LFA reader. The captured image of the strip is extracted for analysis, and CV algorithms are applied to calibrate the image by correcting position, angle, and illumination variations. Adapted with permission from ref. 90. Copyright 2023, *Analyst*.

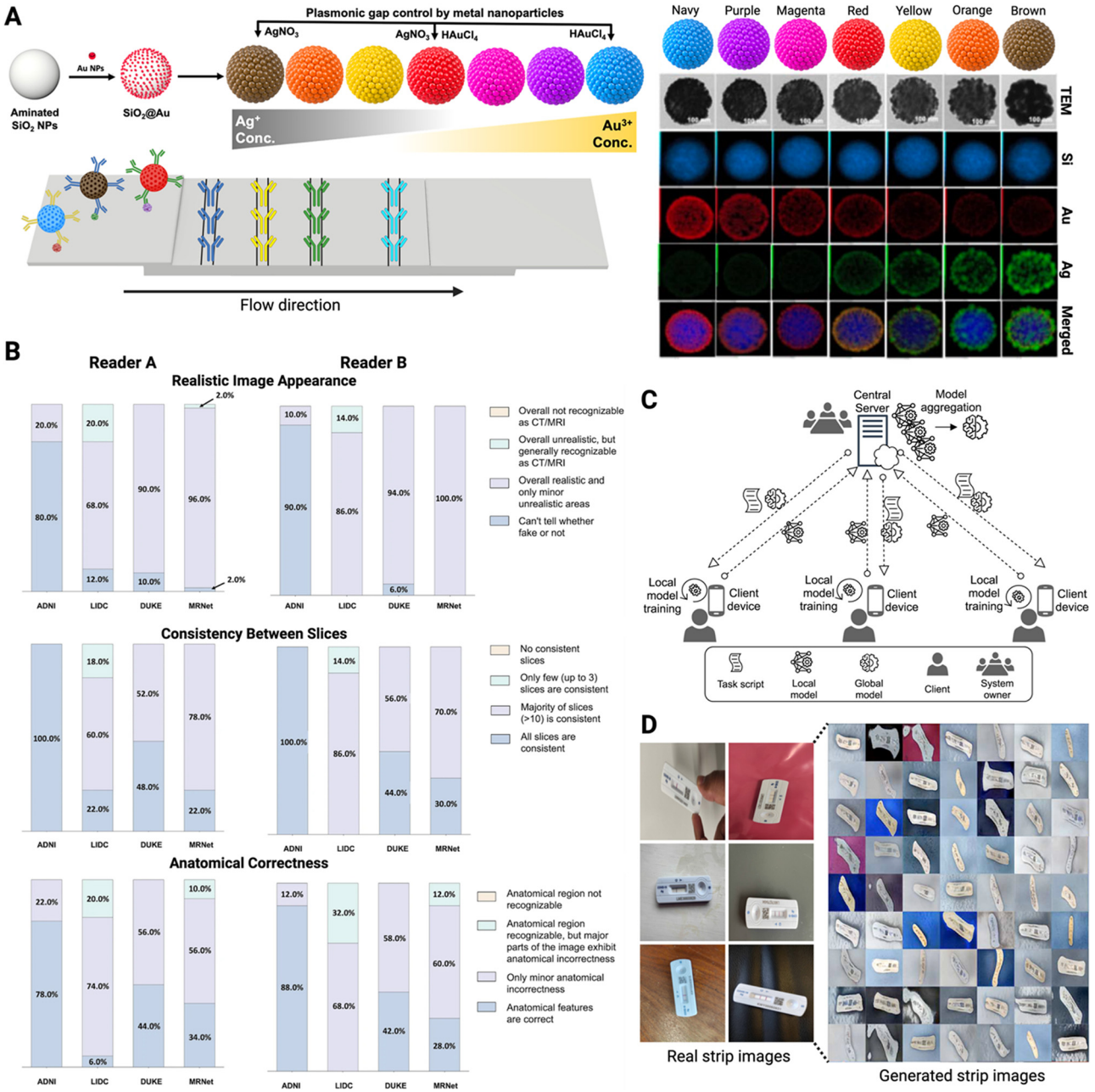

Fig. 4 Possible future applications for enhancing LFA specificity and ML algorithms. (A) New class of multicolored probes (PINs) for LFAs. Depending on the concentration of the metal precursor, 7 kinds of PINs can be fabricated. Using different kinds of PINs, which are conjugated with different antibodies, is utilized for multiplex LFA. Adapted from ref. 88. Copyright 2024, Minsup Shin, Wooyeon Kim, Kwanghee Yoo, Hye-Seong Cho, Sohyeon Jang, Han-Joo Bae, Jaehyun An, Jong-chan Lee, Hyejin Chang, Dong-Eun Kim, Jaehi Kim, Luke P. Lee and Bong-Hyun Jun, published by *Nano Convergence* under the license indicated. (B) Generated medical image quality control using two different radiologists with nine years (reader A) and five years (reader B) of experience in clinical radiology. The images were evaluated based on realistic image appearance, consistency between slices, and anatomical correctness. Both readers were asked to evaluate 50 generated images. This illustrates a validation strategy applicable to synthetic LFA strip image generation for building up strip image datasets. Adapted from ref. 100. Copyright 2023, Firas Khader, Gustav Müller-Franzes, Soroosh Tayebi Arasteh, Tianyu Han, Christoph Haarburger, Maximilian Schulze-Hagen, Philipp Schad, Sandy Engelhardt, Bettina Baeßler, Sebastian Foersch, Johannes Stegmaier, Christiane Kuhl, Sven Nebelung, Jakob Nikolas Kather and Daniel Truhn, published by *Scientific Reports* under the license indicated. (C) Overview of federated learning. Multiple client devices, such as smartphones, perform local model training on their private data without transferring the raw data to a central server. Each client uses a shared task script and updates a local model based on its own data. These local models are then transmitted to a central server, where model aggregation occurs to generate a refined global model. Then, the global model is redistributed to clients for the next training ground. With this architecture, client data are kept private. With this strategy, privacy-preserving LFA image analysis across datasets can be completed without any problem. Adapted with permission from ref. 102. Copyright 2022, *Journal of Systems and Software*. (D) Representative artificially generated images produced by StyleGAN2-ADA using real-time LFA strip images. This model demonstrates LFA strip image dataset generation where limited strip images are available. Adapted from ref. 101. Copyright 2024, Vishnu Pannipulath Venugopal, Lakshmi Babu Saheer and Mahdi Maktabdar Oghaz, published by *Frontiers in Artificial Intelligence* under the license indicated.

Table 2 Summary of ML approaches in LFA applications

Function	Model	Application or target analyte	Performance metrics	References
Quantitative classification	CNN (LeNet-5), SVM, *k*-NN, random forest	COVID-19, SARS-CoV-2 N protein	CNN: 95.8% accuracy SVM/*k*-NN: <83% Random forest: 93.7%	29
Pose correction and quantitative output	Resnet-50 CNN + ViT	COVID-19, SARS-CoV-2 neutralizing antibodies	ViT pipeline > AuNP LFA LoD: 160 ng mL^{-1} Range: 625–10 000 ng mL^{-1}	89
Transfer learning for UCNP LFA	Pretrained CNN with transfer learning	—	Accuracy: 95.7% Sensitivity: 94.3% Specificity: 96.1% 40% faster training	28
Colour ratio regression	Computer vision pipeline + regression	Influenza A and COVID-19, influenza AN protein and SARS-CoV-2 N protein	Accuracy: 95–96% LoD improvement to 0.36–0.40 ng mL^{-1}	90
Test result classification (positive/negative/invalid)	Resnet-50 CNN	HIV, HIV-1 and HIV-2 antibodies	Accuracy: 98.6% Sensitivity: 97.8% Specificity: 99.1%	80
Multi-brand LFA classification	CNN + image preprocessing + transfer learning	COVID-19, SARS-CoV-2 (different LFA kits)	Accuracy: >95% Sensitivity: 93–97% Specificity: 96–99%	79
Multi-test line quantification	Signal processing + regression	Serum amyloid A (SAA)	Accuracy: 94.23%	91
Remote image-based diagnosis	CNN + preprocessing + QR-based data sync	SARS-CoV-2	Accuracy: 98.4% on >5000 labelled images	26
Time-series LFA evaluation	YOLO + CNN + LSTM (TIMESAVER model)	COVID-19, influenza, and non-infectious biomarkers (troponin I and hCG)	Accuracy: 97.6% Sensitivity: 96.3% Specificity: 100% 10× faster than manual	27
At-home LFA test classification	SVM + image processing (ALFA model)	COVID-19, SARS-CoV-2 antibodies	Accuracy: 92.6–98.3% Sensitivity: 90.1–97.1% Specificity: 98.7–99.4%	30

ng mL^{-1} and a dynamic range of 625–10 000 ng mL^{-1}. Strip images were captured with a custom LEGO-based smartphone cradle and analyzed by an ML pipeline that outputs antibody concentration. The algorithm first locates the strip and then quantifies signal intensity, and robust orientation recognition was achieved through a three-stage procedure: (i) background removal and resizing, (ii) feature extraction with a ResNet-50 CNN using group normalization to offset small-batch effects, and (iii) pose prediction with a vision transformer (ViT). The researchers employed training with Adam optimizer with an initial learning rate of 5×10^{-6} (halved every 10 epochs), a weight decay of 1×10^{-4}, and random Gaussian noise augmentation to curb overfitting. Interestingly, the developed ML platform was tested with 50 clinical sera and validated using a commercial ELISA, and it outperformed an AuNP LFA (Fig. 3B).[89]

Both Davis and Tomitaka[29] and Tong *et al.*[89] demonstrated an improved performance over traditional LFAs but with different modeling techniques. Davis and Tomitaka showed that the addition of a LeNet-5-based CNN to a standard AuNP LFA can raise read-out accuracy to 95.8% without changing any hardware. Their binary-antigen approach proves that the compact CNN can tolerate noisy low-resolution images and can translate a yes/no strip into semi-quantitative results useful for population surveillance. In contrast, Tong *et al.* overhauled both the chemistry reporter and the analytics. They replaced the most widely used detection label AuNPs with highly light-absorbing PDA and used a ViT-based pipeline to convert smartphone images into precise neutralizing-antibody concentrations. Additionally, in a different study, an AI-assisted transfer learning approach was applied in the analysis of up-conversion nanoparticle (UCNP)-based LFA signals.[28] UCNPs produce fluorescence emissions with higher signal-to-noise and background noise compared to traditional colorimetry. Therefore, pretrained CNN models were adapted to UCNP image data using transfer learning. The model was trained using a large number of labeled images (approximately 1200) and achieved 95.7% accuracy, 94.3% sensitivity, and 96.1% specificity on the test set. Transfer learning reduced training time by 40% while increasing the model's generalization capacity and reproducibility. This method enables UCNP-based LFAs to perform quantitative analysis with high sensitivity even at low biomarker concentrations, offering a significant improvement in both accuracy and reliability in field applications.[28]

In 2023, Lee *et al.* introduced a computer vision (CV) and a ML pipeline that rebuilds the influenza A and SARS-CoV-2 antigen LFAs to deliver a quantitative read-out on a smartphone. The CV algorithm automatically corrects strip rotation, lateral positioning, and illumination *via* Canny-edge detection, principal component analysis, and white-balance

calibration, then extracts the red/blue ratio of the test line for regression. Across 140 influenza A and 120 SARS-CoV-2 spiked samples, their CV assistance tripled the analytical sensitivity from 0.11 to 0.39 (R^2 = 0.95) for influenza A and from 0.03 to 0.10 (R^2 = 0.96) for SARS-CoV-2, with limits of detection improved to 0.36 ng mL^{-1} and 0.40 ng mL^{-1}, respectively. With this, the researchers denoted that CV/ML optimization alone can elevate the quantitative performance of LFAs, forging a practical path to reliable, equipment-free PoC diagnostics (Fig. 3C).[90] Turbé *et al.* used a smartphone-integrated deep learning (DL) algorithm to reduce errors arising from visual evaluation of LFA-based rapid diagnostic tests for HIV by field users.[80] The image processing process included preprocessing steps such as color correction, geometric alignment, and contrast enhancement of photographs of test cassettes. These images were then classified using a CNN built on the ResNet-50 architecture. The model was able to distinguish positive, negative, and invalid test results; a validation study with field data yielded 98.6% accuracy, 97.8% sensitivity, and 99.1% specificity. What is more is that the model has been shown to make reliable decisions under challenging conditions such as low light and low line density.[80] In a similar study, a rapidly adaptable DL-based analysis system was implemented for the automated and accurate interpretation of SARS-CoV-2 antigen and LFA tests from different manufacturers.[79] This system applies conventional image processing techniques such as geometric correction, segmentation, normalization, and region extraction to test images that were acquired with a smartphone camera, and the processed images are then analyzed using a specifically designed CNN to classify test results. The model achieved over 95% accuracy, 93–97% sensitivity, and 96–99% specificity under field conditions, and using transfer learning the model was able to quickly adapt to different test brands and formats using a small number of new samples. This provided flexibility and broad usage in field applications.[79]

In another research, an algorithm which automatically applies light normalization and alignment was developed for multiplex LFA systems.[91] The algorithm calculates the pixel-based intensities of each test line and performs a quantitative assessment of analyte concentration using signal processing and regression analysis. Specifically, the aim was to capture the nonlinear relationship between the extracted eigenvalues and the concentration values using a support vector machine regression model. This regression model approach minimized the model complexity while maintaining prediction accuracy. This approach demonstrated high robustness across various noise conditions and achieved a strong predictive performance across multiple quantitative analyses. By integrating image processing with the regression model, this method increases the sensitivity of LFA-based tests and enables simultaneous quantitative analysis of multiple biomarkers for infectious diseases such as HIV, HBV and HCV, DENV, ZIKV, and COVID-19, while minimizing user-induced interpretation errors.[91] In another study, a smartphone-based platform with AI support was created to enable digital and remote interpretation of LFA tests for SARS-CoV-2.[26] This platform uses a preprocessing algorithm that automatically aligns the image of the test cassette, correcting color tones, and then analyzes it with CNN, which evaluates the signal intensity of the test and control lines. The model was trained using >5000 labeled images and achieved 98.4% accuracy, eliminating user-dependent subjective errors. Results were transmitted to a central system *via* QR code, ensuring remote monitoring and epidemiological data integrity.[26] This approach represents a significant advance in the digitization of LFA tests and their integration with telemedical systems.

From a different perspective on ML integration, a method called TIMESAVER (time-efficient immunoassay with smart AI-based verification) was developed based on a time-series DL method for evaluating LFA.[27] This model first enables fast and accurate detection of test and control lines using the YOLO algorithm, which is a DL-based object detection algorithm for real-time operation capable of detecting all objects in an image in a single feedforward pass. Then, the model analyzes time-series data using an architecture consisting of CNN and LSTM layers to generate results. The final classification performed through fully connected layers determines test results with high accuracy. In blind tests conducted on COVID-19 clinical samples, the TIMESAVER model achieved 96.3% sensitivity, 100% specificity, and 97.6% accuracy, producing results approximately 10 times faster than human assessment (approximately 1–2 minutes).[27] Similarly, successful results were also achieved in influenza testing.[27] This study demonstrates that integrating DL algorithms into LFA systems can not only increase diagnostic accuracy but also dramatically shorten the time to diagnosis.[27]

Wong *et al.* presented an ML-based system called ALFA (automated lateral flow analysis) to automate the detection of SARS-CoV-2 antibodies using at-home LFA tests.[30] This system was trained on approximately 595 000 LFA test photos taken by users with their smartphones and classifies test results as IgG positive, IgG negative, or invalid. Image processing techniques such as edge detection, segmentation, and color intensity analysis were applied in the image preprocessing phase. SVM, which can handle nonlinear structures, was used for classification. The model demonstrated high concordance with human experts, with Cohen's kappa = 0.90–0.97, and outperformed participants, particularly in correctly identifying weakly positive results. The ALFA system achieved 98.7–99.4% specificity and 90.1–97.1% sensitivity compared to visual assessment. This study strongly suggests that image processing techniques integrated with ML algorithms can increase the sensitivity of home-based LFA tests by reducing user-induced error and enable the production of high-volume, accurate data in public health surveillance.[30] Beyond pathogen detection, ML algorithms have also been explored for the rapid identification of antimicrobial resistance such as carbapenemase enzymes.[92,93] In a world where antibiotic

consumption and multidrug resistance have numerously increased,[92] the detection of antimicrobial resistance represents a significant extension of LFA and thus is a valuable application for preventing infections.[92]

5. Current challenges and future aspects

Despite the widespread adoption and significant benefits of LFAs, several challenges persist: technical limitations, standardization issues, and implementation in low-resource environments.[22,43] In terms of technical limitations, LFAs face constraints related to sensitivity and specificity, often exhibiting higher limits of detection compared to conventional laboratory-based diagnostic methods such as PCR and ELISA. Sensitivity variations across different test brands, as observed in COVID-19 LFAs, demonstrate a broad range of performance (from 34% to 88%), potentially compromising clinical reliability. Additionally, LFAs frequently struggle to differentiate between closely related pathogens due to antigenic similarity as observed in cases like dengue and Zika viruses. Another challenge is the optimization of bioreceptor binding affinities and conjugate release kinetics. These are critical for accurate analyte detection, yet LFAs often exhibited signal variability or false negatives. Sample delivery problems such as the high-dose hook-effect, uneven flow caused by the membrane adhesives, and incorrect placement/gluing of membranes can also produce false readings or anomalous test-line intensities since the detection probe may accumulate between the borders of the membranes. The lack of standardized protocols across different LFA platforms further contributes significantly to the variability in assay performance. Variations in manufacturing processes such as nanoparticle labelling techniques and detection methodologies can lead to inconsistent test outcomes. This inconsistency complicates the direct comparison of the results between different assays, which pose a significant barrier to regulatory approval. Integration of ML algorithms can compensate for visual ambiguity by converting qualitative strip images into quantitative outputs, just like Davis and Tomitaka[29] and Tong *et al.*[89]

Computer-based approaches in disease detection have made impressive outcomes since the COVID-19 pandemic, yet they still face significant limitations in both variety and scope. Many existing studies have primarily focused on respiratory infections such as COVID-19 (ref. 29, 89 and 90) and often neglected a broader comparison with other respiratory and systemic infectious diseases such as influenza or tuberculosis. This narrow focus creates a research gap in understanding the generalizability and robustness of ML models across different pathogens. Further, this emphasis on a narrow slice of pathogens also makes it difficult to judge whether an algorithm that excelled specifically for COVID-19 will generalize to other infectious diseases where line morphology, background colour, and strip materials differ substantially. Another major barrier lies in the availability and quality of datasets. ML models rely heavily on large, diverse, and high-quality datasets for effective training and validation.[30] However, obtaining such datasets is often challenging. Publicly available datasets are frequently limited in scope, suffer from inconsistent labeling, or lack representative diversity across populations and clinical conditions. In contrast, high-quality proprietary datasets are often locked behind paywalls, creating barriers for independent or resource-constrained research groups.[30] Generating a custom dataset is a viable alternative but demands considerable time, financial resources, and ethical clearance. Ethical concerns and privacy still hold a critical role for clinical applications. Smartphone-based LFA readers, which are becoming increasingly common in testing and PoC settings, produce vast amounts of image data, but privacy concerns make it impossible to centralize those photos. In addition, color space optimization should be carefully considered. Actually, the literature demonstrates that the optimal colour space leads to an advantageous colorimetric sensing, particularly in terms of accuracy, precision, dynamic range and robustness against illumination variation.[94]

Finally, ML-assisted LFA readers introduce additional regulatory and translational considerations because digital interpretation complements the conventional biochemical detection step. During the COVID-19 pandemic, several rapid diagnostic and reader-integrated systems obtained authorization from the U.S. Food and Drug Administration (FDA);[95] however, sustained market entry generally requires clearance through established pathways such as the *de novo* route for first-in-class devices[96] or the 510(k) pathway for devices demonstrating substantial equivalence.[97] These pathways necessitate predefined algorithm change management strategies together with robust validation using large, well-curated datasets. In the European Union, ML-supported LFA readers fall within the IVDR framework, where increasing risk classification is associated with stricter requirements for clinical evidence, post-market performance monitoring, and software lifecycle oversight.[98] The transition from the ASSURED (affordable, sensitive, specific, user-friendly, rapid, equipment-free, delivered) to REASSURED (real-time connectivity, ease of specimen collection, plus the original ASSURED) criteria further reflects the growing emphases on connectivity and usability in next-generation PoC diagnostics, providing a guiding framework for digitally readable LFA systems.[99]

Several strategies could close the aforementioned gaps. One potential is the establishment of regionally curated, publicly accessible datasets. By fostering local dataset collection initiatives while ensuring standardized protocols and data privacy, researchers can accelerate model development and validation across a wider range of infectious diseases. This not only democratizes access to critical data but also promotes global collaboration and enables faster responses to emerging public health threats.[30] Synthetic augmentation can further mitigate scarcity. Diffusion models[100] (Fig. 4B) or StyleGANs[101] (Fig. 4D) trained on the anchor set can generate photorealistic strips

that vary illumination, camera angle, and band intensity in controlled ways, which creates examples that rarely appear. These methods can create realistic LFA images to supplement training sets, especially for underrepresented pathogens or test variations. Further pairing with domain-randomized renderers that model membrane texture and colloidal-gold dynamics, synthetic images can help networks to learn to ignore background noise while remaining sensitive to subtle shifts. Privacy-preserving models such as federated learning (FL) can circumvent ethical and privacy concerns by allowing models to be trained directly on local devices such as smartphones or lab computers without transferring the raw image data. Instead, only model weight updates are shared with a central server, which aggregates them to improve the global model (Fig. 4C).[102] This setup preserves user privacy while enabling collaboration across distributed datasets, ultimately improving the generalizability and robustness of LFA image analysis tools. Ultimately, the integration of LFA–ML represents a digital transformation far beyond traditional diagnostic methods in terms of accuracy, reliability, and scalability. This integration lays the foundation for the diagnostic and monitoring infrastructure of the future, both improving individual test quality and enabling the digitalization of public health systems.

The integration of ML algorithms is expected to become essential for enhancing the effectiveness and reliability of LFA-based diagnostic systems in field applications.[31] Supporting image-based analysis through mobile devices enables user-independent, standardized results.[103] This integration can allow LFAs to provide semi-quantitative or even fully quantitative outputs, potentially informing parameters such as infection burden. However, interpretability of the employed ML approaches is pivotal to improve robustness in the integration of ML and LFA systems; for example, it is crucial to verify/demonstrate that the employed ML approach is based on significant signals provided by LFA outcomes rather than the inherent noise. Looking ahead, ML-supported PoC devices are expected to extend beyond diagnostics to broader applications, including treatment monitoring, patient follow-up, outbreak modeling, and AI-driven early warning systems. Furthermore, integrating data sharing with cloud-based infrastructures could play a pivotal role in public health management by enabling rapid analysis of global infection dynamics.

6. Conclusion

LFAs are low-cost tools widely used worldwide for early, rapid, and on-site PoC diagnosis of infectious diseases. However, the accuracy and reliability of these systems still largely depend on the user's visual interpretation, which can lead to false-negative/positive results, particularly at low signal levels, negatively impacting diagnostic quality. These limitations of traditional LFA systems are inherently too complex to be overcome by chemical or biological optimization alone. ML-powered analysis approaches offer a radical solution to these challenges. Image processing algorithms and ML models have made it possible to digitally analyze test lines and measure signal intensity objectively, reproducibly, and with high accuracy. Furthermore, the integration of these systems with smartphones makes advanced diagnostic capabilities accessible even in regions lacking laboratory infrastructure. In this review, we highlighted how the integration of LFA with ML algorithms is transforming PoC diagnostic devices not only into medical decision support systems but also into global infection surveillance systems with large datasets. This transformation is groundbreaking for pandemic preparedness, health equity, and early intervention strategies. Therefore, the construction of biosensor technologies is based not only on biochemistry but also on computational intelligence, which emerges as a new paradigm in the evolution of modern diagnostic sciences.

Conflicts of interest

There are no conflicts to declare.

Data availability

This review does not include any original data. All information presented is derived from previously published literature. No new datasets were generated or analyzed.

Acknowledgements

S. T. acknowledges the TÜBITAK 2232 International Fellowship for Outstanding Researchers Award (118C391), TÜBITAK-1001 Scientific and Technological Research Projects (123S582, 123Z050, 225S122, 125Z215), Alexander von Humboldt Research Fellowship for Experienced Researchers, Marie Skłodowska-Curie Individual Fellowship (101003361), and Royal Academy Newton-Katip Çelebi Transforming Systems Through Partnership Award (120N019) for the financial support of this research. N. A. acknowledges support by EMBO Scientific Exchange Grant (11627) and TÜBITAK-2218 Domestic Postdoctoral Research Scholarship Project (122C195). Opinions, interpretations, conclusions, and recommendations are those of the author and are not necessarily endorsed by the TÜBİTAK. This work was partially supported by the Science Academy's Young Scientist Awards Program (BAGEP), Outstanding Young Scientists Awards (GEBIP), Dr. Nejat Eczacibasi Medicine Incentive Award, IBG Science Medal from Izmir Biomedicine and Genome Center, ELGINKAN Foundation Technology Prize, TGC Sedat Simavi Health Sciences Award, Parlar Foundation Research Incentive Award, Parlar Foundation Technology Incentive Award, and Bilim Kahramanlari Dernegi The Young Scientist Award. This study was conducted using the service and infrastructure of Koç University Translational Medicine Research Center (KUTTAM). E. M.-N. acknowledges the support of the Dirección General de Asuntos del Personal Académico de la Universidad Nacional Autónoma de México (grant PAPIIT-IT100124). E. M.-N. also acknowledges support from Fundación Marcos Moshinsky UNAM (Cátedra Moshinsky

2024) and SECIHTI (grant MADTEC-2025-M-137). The authors have no other relevant affiliations or financial involvement with any organization or entity with a financial interest in or financial conflict with the subject matter or materials discussed in the manuscript apart from those disclosed. For the figures, Biorender was used.

References

1 A. S. Fauci, The global challenge of infectious diseases: the evolving role of the National Institutes of Health in basic and clinical research, *Nat. Immunol.*, 2005, **6**(8), 743–747, DOI: 10.1038/ni0805-743.
2 S. Wang, *et al.*, Emerging and reemerging infectious diseases: global trends and new strategies for their prevention and control, *Signal Transduction Targeted Ther.*, 2024, **9**(1), 223, DOI: 10.1038/s41392-024-01917-x.
3 C. Wang, M. Liu, Z. Wang, S. Li, Y. Deng and N. He, Point-of-care diagnostics for infectious diseases: From methods to devices, *Nano Today*, 2021, **37**, 101092, DOI: 10.1016/j.nantod.2021.101092.
4 H. Sohrabi, *et al.*, Lateral flow assays (LFA) for detection of pathogenic bacteria: A small point-of-care platform for diagnosis of human infectious diseases, *Talanta*, 2022, **243**, 123330, DOI: 10.1016/j.talanta.2022.123330.
5 R. Y. Alhabbab, Lateral Flow Immunoassays for Detecting Viral Infectious Antigens and Antibodies, *Micromachines*, 2022, **13**(11), 1901, [Online], available: https://www.mdpi.com/2072-666X/13/11/1901.
6 A. Zumla and D. S. C. Hui, Emerging and Reemerging Infectious Diseases: Global Overview, *Infect. Dis. Clin. North Am.*, 2019, **33**(4), xiii–xix, DOI: 10.1016/j.idc.2019.09.001.
7 E. Morales-Narváez and C. Dincer, The impact of biosensing in a pandemic outbreak: COVID-19, *Biosens. Bioelectron.*, 2020, **163**, 112274, DOI: 10.1016/j.bios.2020.112274.
8 R. E. Baker, *et al.*, Infectious disease in an era of global change, *Nat. Rev. Microbiol.*, 2022, **20**(4), 193–205, DOI: 10.1038/s41579-021-00639-z.
9 Z. Qu, L. Zhang, Y. Sha, B. Zhang and K. Zhang, Impact of dual climatic and socioeconomic factors on global trends in infectious disease outbreaks, *Sci. Rep.*, 2025, **15**(1), 16092, DOI: 10.1038/s41598-024-83431-2.
10 S. Tasoglu, Toilet-based continuous health monitoring using urine, *Nat. Rev. Urol.*, 2022, **19**(4), 219–230, DOI: 10.1038/s41585-021-00558-x.
11 F. Di Nardo, M. Chiarello, S. Cavalera, C. Baggiani and L. Anfossi, Ten Years of Lateral Flow Immunoassay Technique Applications: Trends, Challenges and Future Perspectives, *Sensors*, 2021, **21**(15), 5185, DOI: 10.3390/s21155185.
12 N. Atceken, M. Munzer Alseed, S. R. Dabbagh, A. K. Yetisen and S. Tasoglu, Point-of-Care Diagnostic Platforms for Loop-Mediated Isothermal Amplification, *Adv. Eng. Mater.*, 2023, **25**(8), 2201174, DOI: 10.1002/adem.202201174.
13 N. Atçeken, D. Yigci, B. Ozdalgic and S. Tasoglu, CRISPR-Cas-Integrated LAMP, (in eng), *Biosensors*, 2022, **12**(11), 1035, DOI: 10.3390/bios12111035.
14 T. P. Mashamba-Thompson, L. T. Pfavayi and F. Mutapi, Blind spots in the implementation of point-of-care diagnostics for underserved communities, *Nat. Rev. Bioeng.*, 2023, **1**(12), 876–878, DOI: 10.1038/s44222-023-00127-4.
15 N. Atceken, I. Bayaki, B. Can, D. Yigci and S. Tasoglu, Mpox disease, diagnosis, and point of care platforms, *Bioeng. Transl. Med.*, 2025, **10**(3), e10733, DOI: 10.1002/btm2.10733.
16 D. Yigci, Ö. Ergönül and S. Tasoglu, Mpox diagnosis at POC, *Trends Biotechnol.*, 2025, **43**(10), 2427–2439, DOI: 10.1016/j.tibtech.2025.04.015.
17 M. Hosseinifard, T. Naghdi, E. Morales-Narváez and H. Golmohammadi, Toward Smart Diagnostics in a Pandemic Scenario: COVID-19, (in English), *Front. Bioeng. Biotechnol.*, 2021, **9**, 637203, DOI: 10.3389/fbioe.2021.637203, Perspective.
18 S. Akbari Nakhjavani, B. K. Tokyay, C. Soylemez, M. R. Sarabi, A. K. Yetisen and S. Tasoglu, Biosensors for prostate cancer detection, *Trends Biotechnol.*, 2023, **41**(10), 1248–1267, DOI: 10.1016/j.tibtech.2023.04.001.
19 M. R. Sarabi, *et al.*, Disposable paper-based microfluidics for fertility testing, *iScience*, 2022, **25**(9), DOI: 10.1016/j.isci.2022.104986.
20 P. Yager, G. J. Domingo and J. Gerdes, Point-of-care diagnostics for global health, (in eng), *Annu. Rev. Biomed. Eng.*, 2008, **10**, 107–144, DOI: 10.1146/annurev.bioeng.10.061807.160524.
21 Z. Rong, *et al.*, Integrated fluorescent lateral flow assay platform for point-of-care diagnosis of infectious diseases by using a multichannel test cartridge, *Sens. Actuators, B*, 2021, **329**, 129193, DOI: 10.1016/j.snb.2020.129193.
22 J. Pedreira-Rincón, *et al.*, A comprehensive review of competitive lateral flow assays over the past decade, *Lab Chip*, 2025, **25**(11), 2578–2608, DOI: 10.1039/D4LC01075B.
23 H. Ijäs, *et al.*, DNA origami signal amplification in lateral flow immunoassays, *Nat. Commun.*, 2025, **16**(1), 3216, DOI: 10.1038/s41467-025-57385-6.
24 N. Younes, *et al.*, A review of rapid food safety testing: using lateral flow assay platform to detect foodborne pathogens, *Crit. Rev. Food Sci. Nutr.*, 2024, **64**(27), 9910–9932, DOI: 10.1080/10408398.2023.2217921.
25 J. Budd, *et al.*, Lateral flow test engineering and lessons learned from COVID-19, *Nat. Rev. Bioeng.*, 2023, **1**(1), 13–31, DOI: 10.1038/s44222-022-00007-3.
26 D. Bermejo-Peláez, *et al.*, A Smartphone-Based Platform Assisted by Artificial Intelligence for Reading and Reporting Rapid Diagnostic Tests: Evaluation Study in SARS-CoV-2 Lateral Flow Immunoassays, (in eng), *JMIR Public Health Surveill.*, 2022, **8**(12), e38533, DOI: 10.2196/38533.
27 S. Lee, *et al.*, Rapid deep learning-assisted predictive diagnostics for point-of-care testing, *Nat. Commun.*, 2024, **15**(1), 1695, DOI: 10.1038/s41467-024-46069-2.
28 W. Wang, K. Chen, X. Ma and J. Guo, Artificial intelligence reinforced upconversion nanoparticle-based lateral flow assay via transfer learning, (in eng), *Fundam. Res.*, 2023, **3**(4), 544–556, DOI: 10.1016/j.fmre.2022.03.025.
29 A. M. Davis and A. Tomitaka, Machine Learning-Based Quantification of Lateral Flow Assay Using Smartphone-

Captured Images, *Biosensors*, 2025, **15**(1), 19, DOI: 10.3390/bios15010019.

30 N. C. K. Wong, *et al.*, Machine learning to support visual auditing of home-based lateral flow immunoassay self-test results for SARS-CoV-2 antibodies, *Commun. Med.*, 2022, **2**(1), 78, DOI: 10.1038/s43856-022-00146-z.

31 G. R. Han, *et al.*, Machine learning in point-of-care testing: innovations, challenges, and opportunities, (in eng), *Nat. Commun.*, 2025, **16**(1), 3165, DOI: 10.1038/s41467-025-58527-6.

32 N. Atceken, A. C. Abdullah, O. Ozarslan, Z. Yıldız and S. Tasoglu, Machine Learning-Augmented Loop-Mediated Isothermal Amplification-Enabled Point-of-Care for Mpox-Specific Detection, *Adv. Intell. Syst.*, 2026, e202500825, DOI: 10.1002/aisy.202500825.

33 M. T. Birtek, V. Aktas, B. Aktas, A. C. Abdullah, A. Ozcan and S. Tasoglu, ML-automated microfluidic circuit design, *Sci. Adv.*, 2026, **12**(5), eaea7598, DOI: 10.1126/sciadv.aea7598.

34 O. Özarslan, *et al.*, Leveraging synthetic imagery and YOLOv8 for a novel colorimetric approach to paper-based point-of-care male fertility testing, *Sens. Diagn.*, 2025, **4**(4), 336–344, DOI: 10.1039/D4SD00348A.

35 S. H. Kim, J. Lee, B. H. Lee, C.-S. Song and M. B. Gu, Specific detection of avian influenza H5N2 whole virus particles on lateral flow strips using a pair of sandwich-type aptamers, *Biosens. Bioelectron.*, 2019, **134**, 123–129, DOI: 10.1016/j.bios.2019.03.061.

36 J. W. Guo, H. Y. Ho, C. Y. Dai, Y. H. Chen, M. L. Yu and L. S. Yu, Single-tube, single-strip lateral flow assays utilizing loop-mediated isothermal amplification for simultaneous hepatitis B and C viral detection, (in eng), *J. Med. Virol.*, 2024, **96**(6), e29721, DOI: 10.1002/jmv.29721.

37 B. Ince and M. K. Sezgintürk, Lateral flow assays for viruses diagnosis: Up-to-date technology and future prospects, *TrAC, Trends Anal. Chem.*, 2022, **157**, 116725, DOI: 10.1016/j.trac.2022.116725.

38 M. T. Birtek, N. Atceken and S. Tasoglu, Programmable 3DP microfluidic bio-reaction system: automated LAMP-on-a-chip, *Lab Chip*, 2025, **25**(21), 5506–5523, DOI: 10.1039/D5LC00003C.

39 N. Atceken, A. Kahya, D. Yigci and S. Tasoglu, CRISPR-on-Chip for Point-of-Care Diagnostics, *ACS Nano*, 2026, **20**(3), 2561–2577, DOI: 10.1021/acsnano.5c19771.

40 N. Atceken, *et al.*, Development and Validation of LAMP Assays for Distinguishing MPXV Clades with Fluorescent and Colorimetric Readouts, *Biosensors*, 2025, **15**(1), 23, DOI: 10.3390/bios15010023.

41 J. He, *et al.*, Rapid detection of SARS-CoV-2: The gradual boom of lateral flow immunoassay, (in English), *Front. Bioeng. Biotechnol.*, 2023, **10**, 1090281, DOI: 10.3389/fbioe.2022.1090281, Review.

42 Y. Peng, Y. Huang, F. Kiessling, D. Renn and M. Rueping, Nanobody-Based Lateral Flow Immunoassay for Rapid Antigen Detection of SARS-CoV-2 and MERS-CoV Proteins, *ACS Synth. Biol.*, 2025, **14**(2), 420–430, DOI: 10.1021/acssynbio.4c00592.

43 H. R. Boehringer and B. J. O'Farrell, Lateral Flow Assays in Infectious Disease Diagnosis, (in eng), *Clin. Chem.*, 2021, **68**(1), 52–58, DOI: 10.1093/clinchem/hvab194.

44 D. R. P. Nicollete, *et al.*, Enhancing a SARS-CoV-2 nucleocapsid antigen test sensitivity with cost efficient strategy through a cotton intermembrane insertion, *Sci. Rep.*, 2023, **13**(1), 4690, DOI: 10.1038/s41598-023-31641-5.

45 Y. Zhang, *et al.*, Recent Progress on Rapid Lateral Flow Assay-Based Early Diagnosis of COVID-19, (in English), *Front. Bioeng. Biotechnol.*, 2022, **10**, 866368, DOI: 10.3389/fbioe.2022.866368, Review.

46 E. Sarathkumar, *et al.*, Enhancing chemical signal transformation in lateral flow assays using aptamer-architectured plasmonic nanozymes and para-phenylenediamine, *Nanoscale*, 2025, **17**(5), 2469–2479, DOI: 10.1039/D4NR04130E.

47 J. Wang, *et al.*, Development of aptamer-based lateral flow devices for rapid detection of SARS-CoV-2 S protein and uncertainty assessment, *Talanta*, 2025, **281**, 126825, DOI: 10.1016/j.talanta.2024.126825.

48 M. Ito, M. Watanabe, N. Nakagawa, T. Ihara and Y. Okuno, Rapid detection and typing of influenza A and B by loop-mediated isothermal amplification: Comparison with immunochromatography and virus isolation, *J. Virol. Methods*, 2006, **135**(2), 272–275, DOI: 10.1016/j.jviromet.2006.03.003.

49 M. Jang, S. Kim, J. Song and S. Kim, Rapid and simple detection of influenza virus via isothermal amplification lateral flow assay, *Anal. Bioanal. Chem.*, 2022, **414**(16), 4685–4696, DOI: 10.1007/s00216-022-04090-8.

50 W. S. Jang, J. M. Lee, E. Lee, S. Park and C. S. Lim, Loop-Mediated Isothermal Amplification and Lateral Flow Immunochromatography Technology for Rapid Diagnosis of Influenza A/B, *Diagnostics*, 2024, **14**(9), 967, DOI: 10.3390/diagnostics14090967.

51 S.-C. Lai, *et al.*, Development of Novel Dengue NS1 Multiplex Lateral Flow Immunoassay to Differentiate Serotypes in Serum of Acute Phase Patients and Infected Mosquitoes, (in English), *Frontiers in Immunology*, 2022, **13**, 852452, DOI: 10.3389/fimmu.2022.852452, Original Research.

52 T. Trakoolwilaiwan, *et al.*, Development of a thermochromic lateral flow assay to improve sensitivity for dengue virus serotype 2 NS1 detection, *Nanoscale*, 2023, **15**(31), 12915–12925, DOI: 10.1039/D3NR01858J.

53 Z. Rong, *et al.*, Smartphone-based fluorescent lateral flow immunoassay platform for highly sensitive point-of-care detection of Zika virus nonstructural protein 1, *Anal. Chim. Acta*, 2019, **1055**, 140–147, DOI: 10.1016/j.aca.2018.12.043.

54 A. T. V. Nguyen, B. T. Duong, H. Park and S.-J. Yeo, Development of a peptide aptamer pair-linked rapid fluorescent diagnostic system for Zika virus detection, *Biosens. Bioelectron.*, 2022, **197**, 113768, DOI: 10.1016/j.bios.2021.113768.

55 X. Bai, *et al.*, Field applicable detection of hepatitis B virus using internal controlled duplex recombinase-aided

amplification assay and lateral flow dipstick assay, *J. Med. Virol.*, 2020, **92**(12), 3344–3353, DOI: 10.1002/jmv.25778.

56 B. Zhang, Z. Zhu, F. Li, X. Xie and A. Ding, Rapid and sensitive detection of hepatitis B virus by lateral flow recombinase polymerase amplification assay, *J. Virol. Methods*, 2021, **291**, 114094, DOI: 10.1016/j.jviromet.2021.114094.

57 S. Tasoglu, *et al.*, Advances in Nanotechnology and Microfluidics for Human Papillomavirus Diagnostics, *Proc. IEEE*, 2015, **103**(2), 161–178, DOI: 10.1109/JPROC.2014.2384836.

58 L. Li, *et al.*, Ready-to-use interactive dual-readout differential lateral flow biosensor for two genotypes of human papillomavirus, *Biosens. Bioelectron.*, 2023, **228**, 115224, DOI: 10.1016/j.bios.2023.115224.

59 H. Xiao, W. Chen, M. Lin, S. Jiang, X. Cui and S. Zhao, Rapid immunoassay for dual-mode detection of HPV16 and HPV18 DNA based on Au@PdPt nanoparticles, *Anal. Methods*, 2024, **16**(13), 1862–1869, DOI: 10.1039/D3AY02307A.

60 R. Zhu, *et al.*, CRISPR/Cas9-based point-of-care lateral flow biosensor with improved performance for rapid and robust detection of Mycoplasma pneumonia, *Anal. Chim. Acta*, 2023, **1257**, 341175, DOI: 10.1016/j.aca.2023.341175.

61 Y. Wang, *et al.*, Development of loop-mediated isothermal amplification coupled with nanoparticle-based lateral flow biosensor assay for Mycoplasma pneumoniae detection, *AMB Express*, 2019, **9**(1), 196, DOI: 10.1186/s13568-019-0921-3.

62 A. L. Tomás, *et al.*, Development of a Gold Nanoparticle-Based Lateral-Flow Immunoassay for Pneumocystis Pneumonia Serological Diagnosis at Point-of-Care, (in English), *Front. Microbiol.*, 2019, **10**, 2917, DOI: 10.3389/fmicb.2019.02917, Original Research.

63 X. Chen, *et al.*, Highly specific and sensitive detection of the Mycobacterium tuberculosis complex using multiplex loop-mediated isothermal amplification combined with a nanoparticle-based lateral flow biosensor, *Braz. J. Microbiol.*, 2021, **52**(3), 1315–1325, DOI: 10.1007/s42770-021-00520-4.

64 K. Chen, J. Zhang and S. Wang, Duplex recombinase aided amplification-lateral flow dipstick assay for rapid distinction of Mycobacterium tuberculosis and Mycobacterium avium complex, (in English), *Front. Cell. Infect. Microbiol.*, 2024, **14**, 1454096, DOI: 10.3389/fcimb.2024.1454096, Original Research.

65 T. Gan, J. Yu, Z. Deng and J. He, ERA-CRISPR/Cas12a system: a rapid, highly sensitive and specific assay for Mycobacterium tuberculosis, (in English), *Front. Cell. Infect. Microbiol.*, 2024, **14**, 1454076, DOI: 10.3389/fcimb.2024.1454076, Original Research.

66 X. Chen, *et al.*, Nanoparticle-Based Lateral Flow Biosensor Integrated With Loop-Mediated Isothermal Amplification for Rapid and Visual Identification of Chlamydia trachomatis for Point-of-Care Use, (in English), *Front. Microbiol.*, 2022, **13**, 914620, DOI: 10.3389/fmicb.2022.914620, Original Research.

67 X. Chen, Q. Zhou, W. Yuan, Y. Shi, S. Dong and X. Luo, Visual and rapid identification of Chlamydia trachomatis and Neisseria gonorrhoeae using multiplex loop-mediated isothermal amplification and a gold nanoparticle-based lateral flow biosensor, (in English), *Front. Cell. Infect. Microbiol.*, 2023, **13**, 1067554, DOI: 10.3389/fcimb.2023.1067554, Original Research.

68 M. D. Avila-Huerta, K. Leyva-Hidalgo, K. Cortés-Sarabia, A. K. Estrada-Moreno, A. Vences-Velázquez and E. Morales-Narváez, Disposable Device for Bacterial Vaginosis Detection, *ACS Meas. Sci. Au*, 2023, **3**(5), 355–360, DOI: 10.1021/acsmeasuresciau.3c00007.

69 WHO, *World malaria report 2024: addressing inequity in the global malaria response*, Geneva, 2024.

70 S.-X. Zhang, *et al.*, Global, regional, and national burden of visceral leishmaniasis, 1990–2021: findings from the global burden of disease study 2021, *Parasites Vectors*, 2025, **18**(1), 157, DOI: 10.1186/s13071-025-06796-x.

71 WHO, *Chagas disease (also known as American trypanosomiasis)*, World Health Organization, https://www.who.int/news-room/fact-sheets/detail/chagas-disease-(american-trypanosomiasis), (accessed 11 July 2025).

72 H. Lin, *et al.*, Rapid Visual Detection of Plasmodium Using Recombinase-Aided Amplification With Lateral Flow Dipstick Assay, (in English), *Front. Cell. Infect. Microbiol.*, 2022, **12**, 922146, DOI: 10.3389/fcimb.2022.922146, Original Research.

73 A. Assefa, *et al.*, Detection of P. malariae using a new rapid isothermal amplification lateral flow assay, *Malar. J.*, 2024, **23**(1), 104, DOI: 10.1186/s12936-024-04928-9.

74 N. J. van Dijk, *et al.*, Simplified molecular diagnosis of visceral leishmaniasis: Laboratory evaluation of miniature direct-on-blood PCR nucleic acid lateral flow immunoassay, *PLoS Neglected Trop. Dis.*, 2024, **18**(5), e0011637, DOI: 10.1371/journal.pntd.0011637.

75 L. M. Peverengo, *et al.*, Novel IgM-based lateral flow assay for diagnosis of congenital Chagas disease, *Infect. Dis.*, 2025, **57**(7), 636–646, DOI: 10.1080/23744235.2025.2468819.

76 G. A. Posthuma-Trumpie, J. Korf and A. van Amerongen, Lateral flow (immuno)assay: its strengths, weaknesses, opportunities and threats. A literature survey, (in eng), *Anal. Bioanal. Chem.*, 2009, **393**(2), 569–582, DOI: 10.1007/s00216-008-2287-2.

77 J. Park, Lateral Flow Immunoassay Reader Technologies for Quantitative Point-of-Care Testing, *Sensors*, 2022, **22**(19), 7398, [Online], available: https://www.mdpi.com/1424-8220/22/19/7398.

78 A. Horta-Velázquez, F. Arce, E. Rodríguez-Sevilla and E. Morales-Narváez, Toward smart diagnostics via artificial intelligence-assisted surface-enhanced Raman spectroscopy, *TrAC, Trends Anal. Chem.*, 2023, **169**, 117378, DOI: 10.1016/j.trac.2023.117378.

79 S. Arumugam, *et al.*, Rapidly adaptable automated interpretation of point-of-care COVID-19 diagnostics, (in eng), *Commun. Med.*, 2023, **3**(1), 91, DOI: 10.1038/s43856-023-00312-x.

80 V. Turbé, *et al.*, Deep learning of HIV field-based rapid tests, (in eng), *Nat. Med.*, 2021, **27**(7), 1165–1170, DOI: 10.1038/s41591-021-01384-9.
81 T. Mahmoudi, T. Naghdi, E. Morales-Narváez and H. Golmohammadi, Toward smart diagnosis of pandemic infectious diseases using wastewater-based epidemiology, *TrAC, Trends Anal. Chem.*, 2022, **153**, 116635, DOI: 10.1016/j.trac.2022.116635.
82 J. Jiao, *et al.*, Development of a Lateral Flow Strip-Based Recombinase-Aided Amplification for Active Chlamydia psittaci Infection, (in English), *Front. Microbiol.*, 2022, **13**, 928025, DOI: 10.3389/fmicb.2022.928025, Original Research.
83 N. Ariffin, *et al.*, Lateral Flow Immunoassay for Naked Eye Detection of Mycobacterium tuberculosis, *J. Sens.*, 2020, **2020**(1), 1365983, DOI: 10.1155/2020/1365983.
84 Y. Xi, C.-Z. Xu, Z.-Z. Xie, D.-L. Zhu and J.-M. Dong, Rapid and visual detection of dengue virus using recombinase polymerase amplification method combined with lateral flow dipstick, *Mol. Cell. Probes*, 2019, **46**, 101413, DOI: 10.1016/j.mcp.2019.06.003.
85 X. Qiu, *et al.*, Instrument-free point-of-care molecular diagnosis of H1N1 based on microfluidic convective PCR, *Sens. Actuators, B*, 2017, **243**, 738–744, DOI: 10.1016/j.snb.2016.12.058.
86 H. Yuan, *et al.*, Centrifugation-assisted lateral flow assay platform: enhancing bioassay sensitivity with active flow control, *Microsyst. Nanoeng.*, 2025, **11**(1), 101, DOI: 10.1038/s41378-025-00923-5.
87 G. Khatmi, *et al.*, Lateral flow assay sensitivity and signal enhancement via laser μ-machined constrains in nitrocellulose membrane, *Sci. Rep.*, 2024, **14**(1), 22936, DOI: 10.1038/s41598-024-74407-3.
88 M. Shin, *et al.*, Highly sensitive multiplexed colorimetric lateral flow immunoassay by plasmon-controlled metal–silica isoform nanocomposites: PINs, *Nano Convergence*, 2024, **11**(1), 42, DOI: 10.1186/s40580-024-00449-y.
89 H. Tong, *et al.*, Artificial intelligence-assisted colorimetric lateral flow immunoassay for sensitive and quantitative detection of COVID-19 neutralizing antibody, *Biosens. Bioelectron.*, 2022, **213**, 114449, DOI: 10.1016/j.bios.2022.114449.
90 S. Lee, *et al.*, Advancing diagnostic efficacy using a computer vision-assisted lateral flow assay for influenza and SARS-CoV-2 detection, *Analyst*, 2023, **148**(23), 6001–6010, DOI: 10.1039/D3AN01189E.
91 S. Zhang, *et al.*, A Quantitative Detection Algorithm for Multi-Test Line Lateral Flow Immunoassay Applied in Smartphones, (in eng), *Sensors*, 2023, **23**(14), 6401, DOI: 10.3390/s23146401.
92 G. A. Ziad, *et al.*, Rapid Identification of Carbapenemase Genes Directly from Blood Culture Samples, *Diagnostics*, 2025, **15**(19), 2480, DOI: 10.3390/diagnostics15192480.
93 J. I. Kim, *et al.*, Machine Learning for Antimicrobial Resistance Prediction: Current Practice, Limitations, and Clinical Perspective, (in eng), *Clin. Microbiol. Rev.*, 2022, **35**(3), e0017921, DOI: 10.1128/cmr.00179-21.
94 A. Horta-Velázquez, G. Ramos-Ortiz and E. Morales-Narváez, The optimal color space enables advantageous smartphone-based colorimetric sensing, *Biosens. Bioelectron.*, 2025, **273**, 117089, DOI: 10.1016/j.bios.2024.117089.
95 FDA, Coronavirus (COVID-19) Update: FDA Authorizes First Machine Learning-Based Screening Device to Identify Certain Biomarkers That May Indicate COVID-19 Infection, U.S. Food and Drug Administration, https://www.fda.gov/news-events/press-announcements/coronavirus-covid-19-update-fda-authorizes-first-machine-learning-based-screening-device-identify, (accessed 27.02.2026).
96 FDA, De Novo Classification Request, U.S. Food and Drug Administration, https://www.fda.gov/medical-devices/premarket-submissions-selecting-and-preparing-correct-submission/de-novo-classification-request, (accessed 27.02.2026).
97 FDA, Premarket Notification 510(k), U.S. Food and Drug Administration, https://www.fda.gov/medical-devices/premarket-submissions-selecting-and-preparing-correct-submission/premarket-notification-510k, (accessed 27.02.2026).
98 EU, Guidance on Classification Rules for in vitro Diagnostic Medical Devices under Regulation (EU) 2017/746, 2025, [Online], available: https://health.ec.europa.eu/document/download/12f9756a-1e0d-4aed-9783-d948553f1705_en?filename=md_mdcg_2020_guidance_classification_ivd-md_en.pdf.
99 K. J. Land, D. I. Boeras, X.-S. Chen, A. R. Ramsay and R. W. Peeling, REASSURED diagnostics to inform disease control strategies, strengthen health systems and improve patient outcomes, Nature, *Microbiology*, 2019, **4**(1), 46–54, DOI: 10.1038/s41564-018-0295-3.
100 F. Khader, *et al.*, Denoising diffusion probabilistic models for 3D medical image generation, *Sci. Rep.*, 2023, **13**(1), 7303, DOI: 10.1038/s41598-023-34341-2.
101 V. Venugopal, L. Saheer and M. Maktabdar Oghaz, COVID-19 lateral flow test image classification using deep CNN and StyleGAN2, *Front. Artif. Intell.*, 2024, **6**, 1235204, DOI: 10.3389/frai.2023.1235204.
102 S. K. Lo, Q. Lu, L. Zhu, H.-Y. Paik, X. Xu and C. Wang, Architectural patterns for the design of federated learning systems, *J. Syst. Softw.*, 2022, **191**, 111357, DOI: 10.1016/j.jss.2022.111357.
103 D. Yigci, *et al.*, Smart sanitary hardware for health monitoring, *npj Biosens.*, 2026, **3**(1), 8, DOI: 10.1038/s44328-025-00074-7.
104 L. Chen, *et al.*, A rapid point-of-care test for dengue virus-1 based on a lateral flow assay with a near-infrared fluorescent dye, *J. Immunol. Methods*, 2018, **456**, 23–27, DOI: 10.1016/j.jim.2018.02.005.
105 S. M. Storms, J. Shisler, T. H. Nguyen, F. A. Zuckermann and J. F. Lowe, Lateral flow paired with RT-LAMP: A speedy solution for Influenza A virus detection in swine, *Vet. Microbiol.*, 2024, **296**, 110174, DOI: 10.1016/j.vetmic.2024.110174.

106 J. Zhang, *et al.*, An HRP-labeled lateral flow immunoassay for rapid simultaneous detection and differentiation of influenza A and B viruses, *J. Med. Virol.*, 2019, **91**(3), 503–507, DOI: 10.1002/jmv.25322.

107 S.-K. Kim, H. Sung, S.-H. Hwang and M.-N. Kim, A New Quantum Dot-Based Lateral Flow Immunoassay for the Rapid Detection of Influenza Viruses, *BioChip J.*, 2022, **16**(2), 175–182, DOI: 10.1007/s13206-022-00053-4.

108 A. E. V. Hagström, *et al.*, Sensitive Detection of Norovirus Using Phage Nanoparticle Reporters in Lateral-Flow Assay, *PLoS One*, 2015, **10**(5), e0126571, DOI: 10.1371/journal.pone.0126571.

109 B. Gleeson, *et al.*, Development of a Novel Fluorescent-Based Lateral Flow Assay for the Detection of Neisseria gonorrhoeae at the Point of Care, *Sex. Transm. Dis.*, 2024, **51**(3), 186–191, DOI: 10.1097/olq.0000000000001913.

110 Z. Zhan, S. He, Y. Cui, J. Yang and X. Shi, Development of a multiplex recombinase polymerase amplification coupled with lateral flow dipsticks for the simultaneous rapid detection of Salmonella spp., Salmonella Typhimurium and Salmonella Enteritidis, *Food Qual. Saf.*, 2024, **8**, fyad059, DOI: 10.1093/fqsafe/fyad059.

111 L. Lin, J. Guo, H. Liu and X. Jiang, Rapid Detection of Hepatitis B Virus in Blood Samples Using a Combination of Polymerase Spiral Reaction With Nanoparticles Lateral-Flow Biosensor, (in English), *Front. Mol. Biosci.*, 2021, **7**, 578892, DOI: 10.3389/fmolb.2020.578892, Original Research.

112 S. W. Kim, *et al.*, Ultra-Sensitive Aptamer-Based Diagnostic Systems for Rapid Detection of All SARS-CoV-2 Variants, *Int. J. Mol. Sci.*, 2025, **26**(2), 745, DOI: 10.3390/ijms26020745.

113 N. Sadeghi, N. Shirazi, M. Dehbashi, B. Maleki, W. C. Cho and Z. Hojati, Development of a rapid LFA test based on direct RT-LAMP for diagnosis of SARS-CoV-2, *Pract. Lab. Med.*, 2024, **42**, e00437, DOI: 10.1016/j.plabm.2024.e00437.

114 J. Kim, *et al.*, Novel Isothermal Amplification Integrated with CRISPR/Cas13a and Its Applications for Ultrasensitive Detection of SARS-CoV-2, *ACS Synth. Biol.*, 2025, **14**(2), 463–469, DOI: 10.1021/acssynbio.4c00605.

115 J. M. Vindeirinho, *et al.*, RT-RAA with a lateral flow assay readout based on ssDNA hybridization for detection of RNA viruses – the case of SARS-CoV-2, *Sens. Actuators, B*, 2025, **426**, 136864, DOI: 10.1016/j.snb.2024.136864.

116 P. Rungkamoltip, *et al.*, Rapid and ultrasensitive detection of circulating human papillomavirus E7 cell-free DNA as a cervical cancer biomarker, *Exp. Biol. Med.*, 2021, **246**(6), 654–666, DOI: 10.1177/1535370220978899.

117 K. Zhang, *et al.*, RPA-CRISPR-Cas-Mediated Dual Lateral Flow Assay for the Point-of-Care Testing of HPV16 and HPV18, *Bioconjugate Chem.*, 2024, **35**(11), 1797–1804, DOI: 10.1021/acs.bioconjchem.4c00375.

118 J. Wang, *et al.*, Dual-OR Logic-Gated Lateral Flow Strip Assay Based on Colorimetric-Fluorescence Dual Indication for Screening of HPV16/18 in Multiple Scenarios, *Anal. Chem.*, 2025, **97**(5), 2963–2971, DOI: 10.1021/acs.analchem.4c05778.

119 M. Lin, *et al.*, Dual lateral flow assay based on PdRu nanocages for human Papillomavirus detection, *J. Colloid Interface Sci.*, 2024, **673**, 893–900, DOI: 10.1016/j.jcis.2024.06.002.

120 Z. Xu, J. Su, Z. Du, K. Wang, F. Xiao and L. Luo, Quantitative measurement of hepatitis B surface antigen using laser-assisted lateral flow assay, *Sens. Biosensing Res.*, 2024, **44**, 100646, DOI: 10.1016/j.sbsr.2024.100646.